Escuela de Caminos
Escuela Técnica Superior de Ingenieros de Caminos, Canales y Puertos
UPC BARCELONATECH

TRABAJO FINAL DE MASTER

A STUDY OF JET-GROUT COLUMN DIAMETER EVALUATION TECHNIQUES

Trabajo realizado por:

Federico Graziani

Dirigido por:

Marcos Arroyo Alvarez de Toledo

Máster en:

Ingeniería del Terreno

Barcelona, **14/06/2019**

Departamento de **Ingeniería civil y ambiental**

ABSTRACT

This work compares three different analytical methods for the prediction of the jet grouting column diameter. In the first part, a general description of the jet grouting technique and an overview of existing quality control methods (both direct and indirect) for diameter is presented. The analytical methods of Carnevale, Flora and Shen are then exposed before showing their application to a real case: the Rijeka's port expansion. Finally, a comparation between the predictions obtained by the different methods and the values deduced from quality control is made and some conclusions are drawn.

INDEX

1 INTRODUCTION *3*

2 QUALITY CONTROL FOR JET GROUTING COLUMNS *4*

2.1 DIRECT METHODS 5

2.2 INDIRECT METHODS 6

3 ANALYTIC PREDICTION MODELS FOR COLUMN DIAMETER *8*

3.1 METHOD 1: CARNEVALE 9

3.2 METHOD 2: FLORA 12

3.3 METHOD 3: SHEN 16

4 DESCRIPTION OF THE CASE STUDY *21*

4.1 OVERVIEW 21

4.2 GEOTECHNICAL CONDITIONS 22

4.2.1 GROUND UNITS 22

4.2.2 GEOTECHNICAL PROPERTIES 23

4.3 JET GROUTING TREATMENT 28

4.3.1 MOTIVATION AND LAYOUT 28

4.3.2 MONITORING DURING EXECUTION 30

4.4 QUALITY CONTROLS 32

4.4.1 CROSS-HOLE ERT METHOD 33

4.4.2 CROSS-HOLE SEISMIC METHOD 35

4.4.3 RESULTS 38

5 APPLICATION OF DIAMETER PREDICTION METHODS TO THE RIJEKA CASE *40*

5.1 METHOD 1 40

5.2 METHOD 2 43

5.3 METHOD 3 46

6 ANALYSIS *52*

6.1 COMPARISON BETWEEN METHODS 52

6.2 COMPARISON WITH ERT AND SEISMIC RESULTS 54

7 CONCLUSIONS *54*

8 REFERENCES..... 55

1 INTRODUCTION

Jet grouting is a soil improvement technique used worldwide, with increasing importance since its inception 50 years ago.
The jet grouting technology (described in detail by Croce et al. 2017) is based on the high-pressure injection of one or more fluids (grout, air, water) into the subsoil. The fluids are injected through small-diameter nozzles placed on a pipe that, in most applications, is first drilled into the soil and is then raised towards the ground surface during jetting. The whole process in shown in Figure 1.
The injected water-cement (W-C) grout cures underground, eventually producing a body made of cemented soil. Most of the time, the treated volume in one injection operation has a quasi-cylindrical shape and is thus named 'jet-grouted column' or simply 'jet column'. These columns are then usually arranged in groups to create treated soil structures, like slabs, tunnel canopies, etc.
Jet grouting injection is accomplished through the so-called 'jet grouting string'. The string is made by jointed rods provided with single, double or triple inner conduits, that convey the fluids to a tool, named 'monitor', mounted at the end of the string. The monitor is provided with one or more small diameter nozzles, designed to transform the high-pressure fluid flow in the string into high-speed jets.
Different procedures can be chosen by selecting a proper combination of drilling and grouting. Usually, both operations are performed by using the same rig, which is able to regulate the rotation and translation of the jet grouting string and monitor.

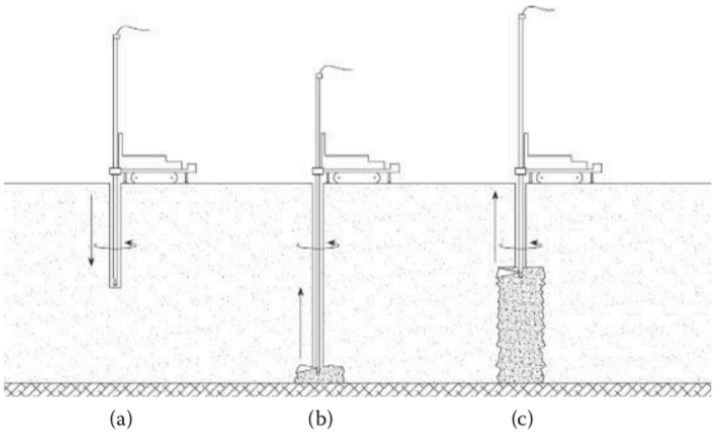

Figure 1 Typical jet grouting procedure: (a) drilling; (b and c) jet column formation (Croce et al. 2017)

Drilling is executed, up to the maximum desired depth of treatment, by using a rotating or rotary-percussive direct drilling system. The bit is mounted at the tip of the monitor and is slightly larger than the pipe string, thus leaving an anular space between the pipe and the borehole wall. The borehole diameter usually ranges between 120 and 150 mm, but, in some cases, it may be as large as 300 mm. Drilling can be performed with air, water, grouts or foams as flushing media.
Jetting is then performed through one or more nozzles placed on the monitor, which is rotated and raised back. The soil is remoulded by the jet action, and part of the injected fluids and of the soil rise to the surface through the gap between the pipe string and the borehole wall, forming a sort of mud that is usually called 'spoil'.

Jet grouting may be executed using different injection systems:

-In the single fluid system, a W-C grout is injected into the ground through one or more nozzles. In this case, soil remoulding and subsequent cementation are both caused by the same fluid.

-In the double fluid system, soil disaggregation and cementation are still carried out by just one fluid, the W-C grout, but the jet of grout is shrouded by a coaxial jet of air, to enhance its effectiveness by concentrating the flow. Such an air jet is provided through a coaxial annular nozzle placed around the grout nozzle.

-In the triple fluid system, soil remoulding and cementation addition are clearly separated. In particular, soil disaggregation is induced by a high-velocity water jet, provided through a nozzle placed on the upper part of the monitor. This water jet is shrouded by a coaxial air jet, supplied by an annular nozzle similar to the one used for the double system. The W-C grout is then delivered from a separate nozzle placed on the lower part of the monitor. In this case, the only purpose of the grout is to deliver cement into the soil previously remoulded by the water jet and, therefore, is delivered at a lower velocity.
A variation of the conventional triple fluid method consists of injecting both water and grout at a very high speed so that the soil is subjected to two subsequent erosion stages (Shen et al. 2009), which could further enhance the treatment radius.

A relevant problem for this technique is the difficulty to predict the geometry (diameter) of the column, as it depends on complex soil-fluid interactions. A related problem is that it is also difficult to check later the characteristics –not just geometry, also material properties- of the executed work - below the surface. These problems are quite central to the technique and have resulted in very intense recent research work on the topic, with many ideas being currently proposed.

Within this context, this work uses detailed field data from an important case-history the port of Rijeka, Croatia- to compare and evaluate three recently proposed different analytical prediction models of jet grout column diameter.

In chapter 2 and 3, the descriptions of methods for quality control for the diameter of jet grouting columns and the analytical prediction models are presented.
Chapter 4 is about the case studied of the port of Rijeka, with a complete description of geotechnical soil and instrumentation parameters, and the results obtained from quality controls for the diameter of the jet grouting columns.
The results obtained from the analytical prediction models and an analysis between the methods described before, are presented in chapter 5 and 6.

2 QUALITY CONTROL FOR JET GROUTING COLUMNS

The different control methods are presented according to the following main purposes (Croce et al. 2017):
• To ensure that the basic materials adopted for jet grouting possess adequate characteristics
• To check that the construction procedure is correctly carried out and that the equipment is working properly
• To quantify the dimensions and properties of the jet-grouted elements
• To verify the performance of jet-grouted structures
• To monitor the jet grouting effects on the surrounding environment and structures

Since this work is about the prediction of diameter, only the geometry control is described: its importance is due to the usual mistake of assuming that the column will be executed with a pre-determined diameter, ignoring possible problems during the execution. Different techniques have been developed to measure the column's diameter, divided into direct and indirect methods.

2.1 DIRECT METHODS

The ideal direct method for the field trials consists in the exposition of the columns (Figure 2). There is no better method because it is possible to measure it directly and observe every production defect. However, it is not always possible to do so, being the method very invasive, and it can be done only during field tests, at limited depth and without the presence of water in the excavation (using well-points would be very expensive) (Croce et al. 2017).

Figure 2 direct measurement of the diameter of discovered vertical columns (Croce et al. 2017)

describing the measurement of diameter in trial horizontal columns executed within the cross-section of a tunnel under construction (Figure 3). In this case, the field trial can be performed with minimum cost, and measurements on the trial columns may be used to continuously control the effectiveness of performed treatments.

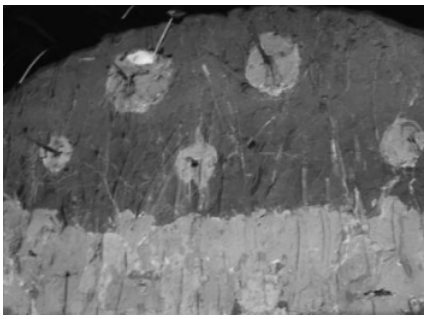

Figure 3 Measurement of the diameter of horizontal trial columns at the excavation front during tunnelling (Croce et al. 2017)

A less invasive direct technique based on the use of a calliper (Figure 4a) having two arms that can be opened by increasing the pressure within a central hydraulic jack (Langhorst et al. 2007). The measurement consists of inserting the tool at different levels into the freshly injected column, varying the pressure of the fluid contained in the jack and measuring the corresponding variation of volume in the jack chamber. The pressure–volume relationship is sensitive to the resistance offered by the surrounding material to the expansion of the two arms, and thus, a sharp deviation from the previous trend, with an increase in resistance, is noticed when the arms reach the undisturbed soil. The measurements reported in Figure 4b shows repetitive results as a proof of the efficiency of the system. There is certainly a problem related to the difficulty of inserting the calliper exactly along

the jet-grouted axis: a misalignment would result in a measurement that is likely smaller (of an unknown quantity) than the true diameter.

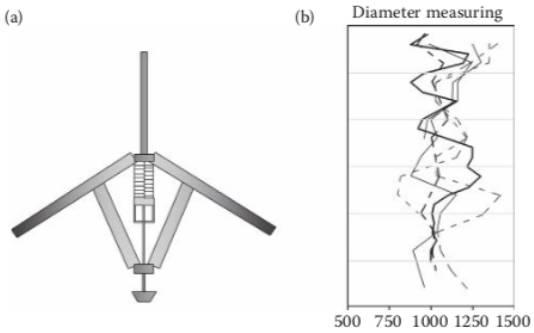

Figure 4 Calliper for the measurement of column diameter (a) and typical results (b). (Modified from Langhorst, O. S. et al., Design and validation of jet grouting for the Amsterdam Central Station. Geotechniek, Special Number on Madrid 14th ECSMGE: pp. 20–23, 2007.)

2.2 INDIRECT METHODS

Indirect methods allow to measure the diameter of the column through the observation of other parameters.
They are the most common methods and can be used in field trials and during the realization.
Examples of indirect measuring techniques (Croce et al. 2017) based on the observation of the effects of jet grouting within inspection holes placed at different distances and parallel to the centreline of columns are reported in Figure 5. The monitoring holes are positioned at variable distances around the injection hole to check if the jet is able to cover the mutual distance at variable depths (Figure 5a, b).
Figure 5b and c show the method of inserting painted small diameter pipes along the measuring verticals, which can be retrieved after treatment to observe if the jet action has reached the pipe, thus removing the paint.
Another interesting application that considers the detection of temperature variations (Figure 5d) (Ho et al. 2001, as reported by Katzenbach et al. 2001; Meinhard et al. 2010) consists in cement hydration produces heat, and the variations (increase and subsequent decrease) of temperature can be linked to the diameter of the column.
More sophisticated controls can be also carried out in the holes.
An example of a more sophisticated method, an interesting method consists in registering the noise generated by the impact of the jet on one or more pipes (Figure 5e). With this method, the pipes are filled with water, and the noise is recorded by some hydrophones (Langhorst et al. 2007). The amount of energy emitted from the passing jet is transformed into an analogue electrical signal, whose power allows an estimation of the distance between the hydrophone and the jet. In all these methods, it is fundamental to have inspection holes parallel to the columns or, better, to know their position with sufficient precision; otherwise, measurements will be affected by significant (and unknown) errors, which would result in only qualitative information. To this aim, a measurement of their inclination is recommended, which, however, makes the measurement more expensive.

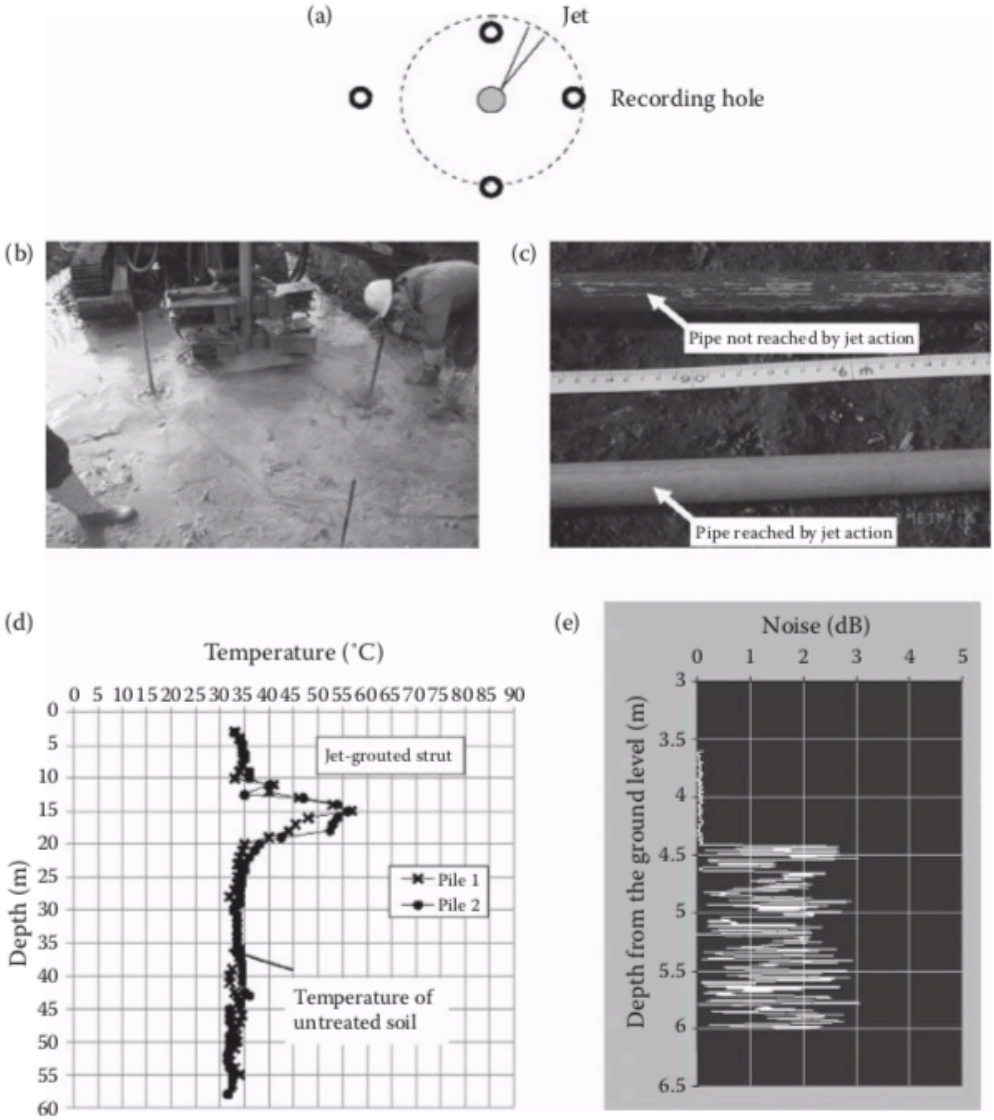

Figure 5 Measurement of column diameter from inspection holes (a) geometric scheme; (b) and (c) visual inspection; (d) temperature; (e) noise recorded by hydrophones (Croce et al. 2017)

A rather popular indirect technique is the 'sonic logging test' (ASTM D5753-e1 2012) carried out into a borehole created along the axis of the hardened column. Figure 6 reports the scheme of a sonic measuring device into a hardened jet-grouted column and its working principle: sonic waves are generated by a source; when they hit the boundary between the treated and the undisturbed soil, waves are reflected and arrive at the receiver after time intervals Δt that depend on the distance Δz (usually of ~1 m), on the diameter of the column D(z) and on the wave velocity (v) in the jet-grouted soil. Then, it is simple to demonstrate that, once v (which has to be previously measured in the laboratory on samples cored from the borehole) and Δz (which is imposed by the operator) are known and Δt is measured, the diameter can be calculated as

$$D = \sqrt{(v \cdot \Delta t)^2 - \Delta z^2} \tag{1}$$

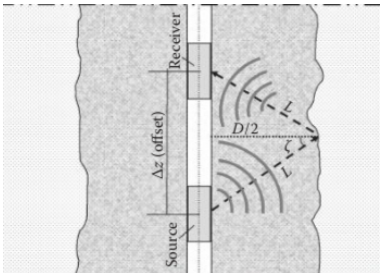

Figure 6 Scheme of sonic indirect measurement of the diameter D of a jet-grouted column (Croce et al. 2017)

Measurements can be made with a predetermined frequency by sliding the probe into the hole (intervals of 2–3 cm are typically adopted). The use of an appropriate acquisition and data processing instrumentation allows the return of almost continuous information along the column axis.
Using this working principle, more refined measurements can be obtained, carrying out a tomography of the physical properties of the jet- grouted column. Whatever the generated signal (electric, acoustic, etc.), the common principle is that a wave is triggered from a source and recorded by a sequence of receivers, all placed within the same borehole placed at the centre of the column. Figure 7 shows the example of electrical resistivity tomography.

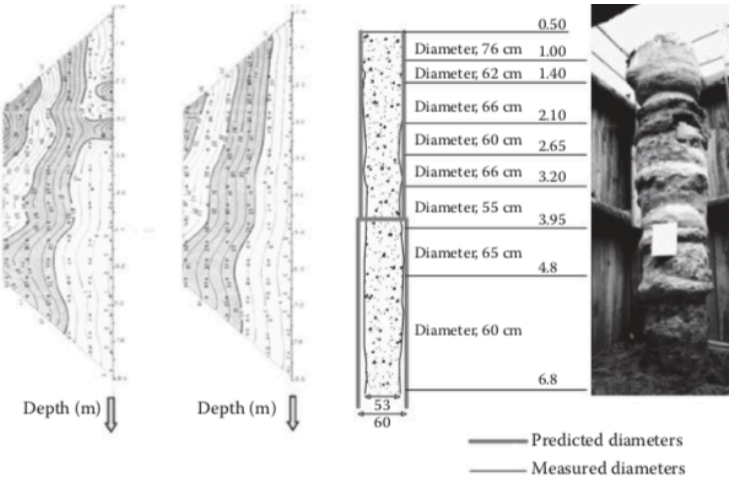

Figure 7 Measurement of column diameter with electrical resistivity tomography. (From Arroyo, M. et al., Informes Sobre Tratamientos de Jet Grouting. ADIF LAV Madrid-Barcelona-Francia, Tramo Torrasa-Sants. Report of the Universidad Politecnica de Catalunya [in Spanish], 110 pp., 2007.)

A much more reliable result can be obtained if the tomography is carried out using more than one borehole placed outside the treated volume.

3 ANALYTIC PREDICTION MODELS FOR COLUMN DIAMETER

During the last years several analytic prediction models for the determination of column diameter in jet grout have been proposed. In this chapter, three different analytic prediction models are described: Carnevale et al. (2012), Flora et al. (2013) and Shen et al. (2013), present the theory behind each of them as well as validation examples.

All these methods can predict the diameter of the jet grouting column and can be simply evaluated with Excel. To predict diameter the inputs required are soil characteristics and jet execution parameters. The inputs are different from each method as will be described in the following.

3.1 METHOD 1: CARNEVALE

The first method analyzed is the one proposed by Carnevale et al. (2012): this one is probably the most ambitious of the three methods examined, because it can evaluate not just the column diameter, but the spoil volume, the dispersed volume and the spoil and column unit weight too (Table 1).

Summarizing the method: it used as input the kind of jet grouting used (monofluid, bifluid or trifluid), some parameters of the planned injection procedure (nozzle diameter, pump pressure…) and some parameters of the ground.
The method is based on some theory concepts of soil mechanics and fluids distribution. It also introduces some empirical correction coefficients for the machine and soil parameters.
As for the analytic calculation part for the diameter of the column it was considered the available energy used by the machine and the soil strength (the more strength of the soil, the more energy will be used for the execution of the column). The grout injected at big pressure will cause the soil's erosion.
Depending on the characteristics of the soil, the injected grout can follow three different paths: remain in site forming the column, permeate through the surrounding soil or return to the surface as spoil through the anular space between the rod and the hole.
The balance between these three components results from the geotechnical characteristics of the soil and of the injection method used.
The method is applicable to the three types of jet grouting, monofluid (only grout), bifluid (grout and air) or trifluid (grout, air and water).
The only part of interest for this thesis is the one of the calculations of the diameter, so only the B part of the model will be considered, as shown in the Table 2.

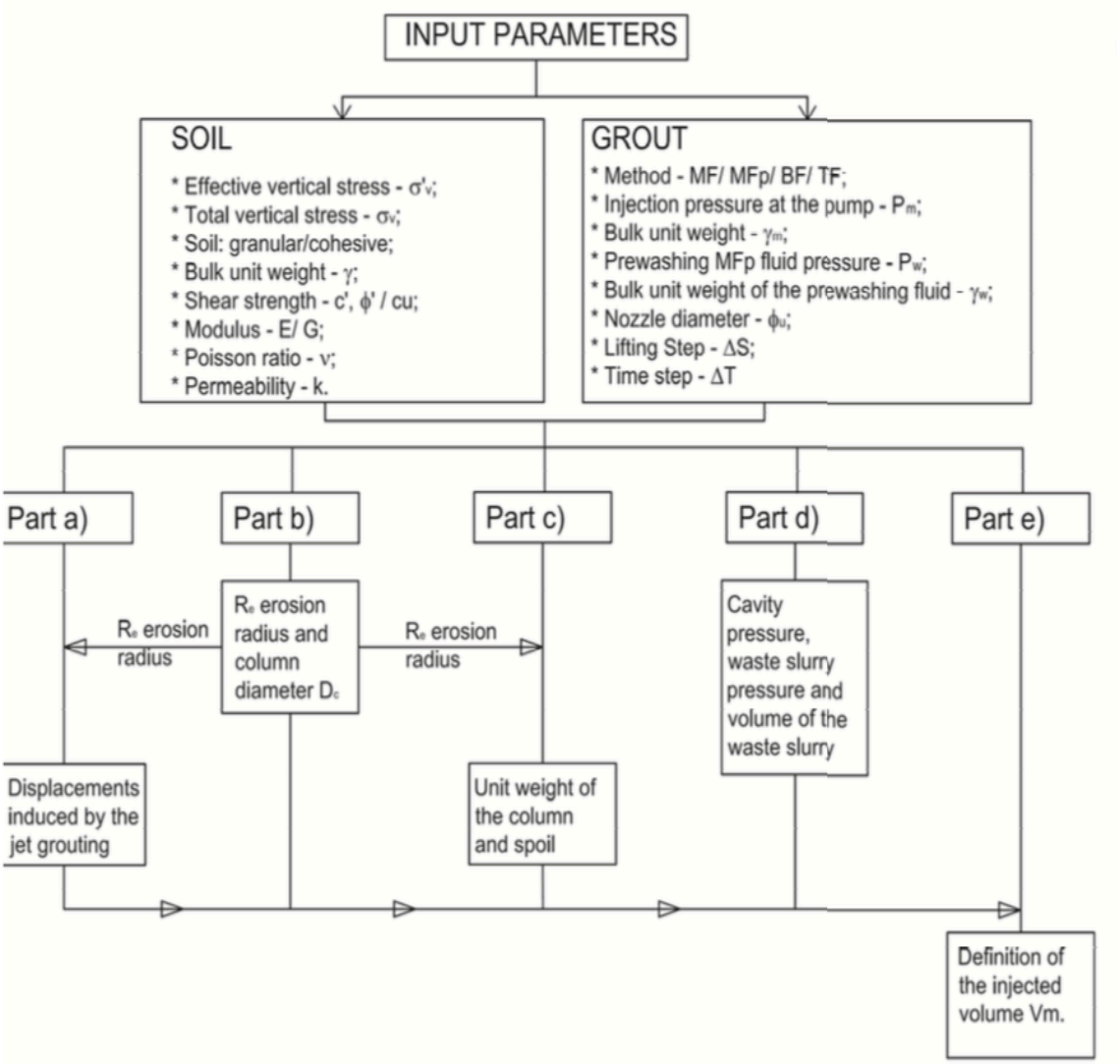

Table 1 method summarized (Carnevale et al. 2012)

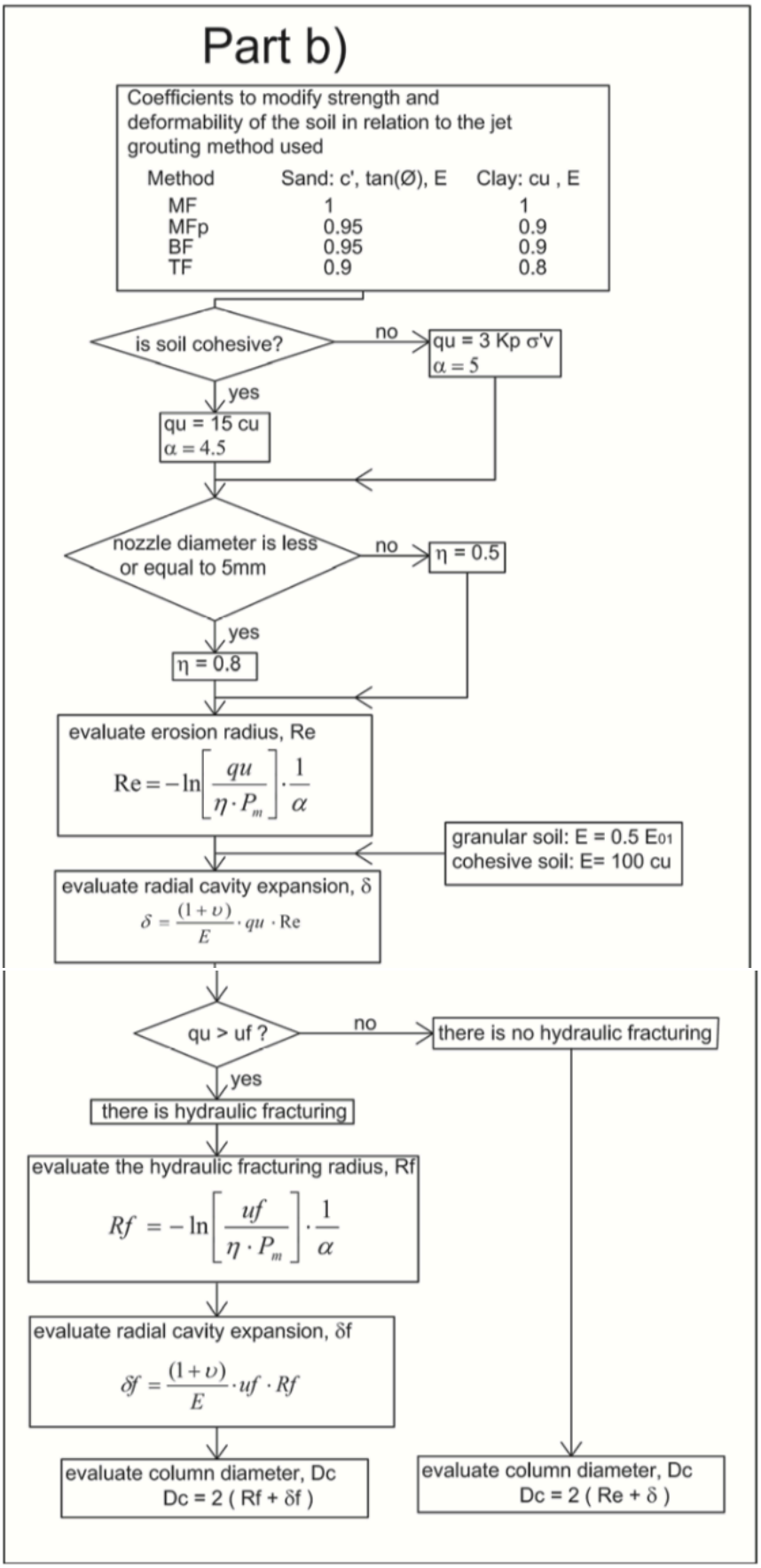

Table 2 Part B for the calculation of the column's diameter (Carnevale et al. 2012)

The pressure of the grout at the nozzle *Pn* decreases with the horizontal distance x from the nozzle. The soil erosion will continue as long as the pressure is higher than the soil resistance qu.
The distance "x" where the injected pressure is equal to the soil resistance qu is called the erosion radius *Re*.
Different soil resistance values are assumed depending on the type of soil (granular or cohesive). Soil resistance can be evaluated with common methods like CPTu or laboratory tests.
After the erosion stops the cylindric cavity will still expand under active pressure. The soil beyond the erosion radius plastifies and the cavity radius will increase with horizontal displacement δ.
Within these conditions, the column diameter will be calculated as:

$$D_c = 2(R_e + \delta) \tag{2}$$

This process is limited by the possibility of localized (plane) hydraulic fracturing. If the cavity pressure is higher than the hydraulic fracturing pressure (u_f), the column diameter will increase and will be evaluated as:

$$D_c = 2\left(R_f + \delta_f\right) \tag{3}$$

with R_f as the distance where the cavity pressure is equal to u_f and δ_f is the cavity expansion at a distance R_f under the pressure u_f.
As often u_f is less than qu, the column diameter Dc_f is higher than Dc.
Two correction coefficients (α for soil type and η for nozzle type) are used to determine the hydraulic losses during injection: their values are taken from Shibazaki (2003) and field observations.

In summary, to predict the column diameter with Carnevale method the required inputs are effective stress σ'_v, passive earth pressure Kp, undrained shear strength Cu, nozzle diameter d_0, pump pressure Pm and elastic modulus E.

3.2 METHOD 2: FLORA

The method reported by Flora et al. (2013), differently from the one of Carnevale, only calculates the diameter of the column, considering the erosion energy of the jet and the soil resistance.
Instead of considering separately the air flow's energy covering the erosion flow, a new parameter is introduced, which represents the beneficial effect of air in reducing the energy dissipation in the exterior surface of the jet.
The submerged jet energy is expressed in terms of longitudinal and transversal velocity. At the exit of the nozzle the flows are parallel, with an initial velocity v_0 constant. As the flow advances, the velocity reduces due to the interaction between the jet and the surrounding fluid. At a distance xc from the nozzle, the velocity reduction affects all the flows produced. The transversal velocity creates a bell-shaped curve of velocities, expanding and flattening as it moves away from the nozzle (Figure 8).

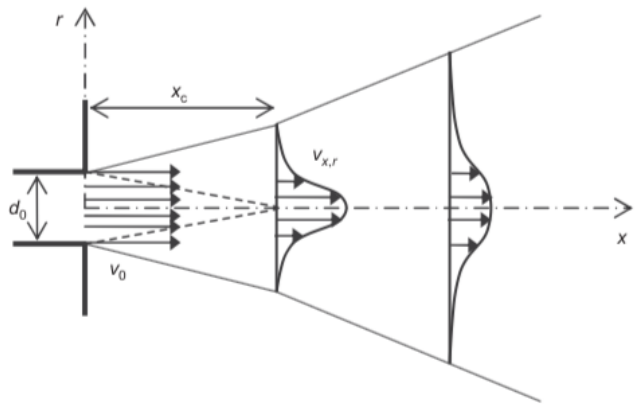

Figure 8 Transverse velocity profiles of a submerged jet (adapted from Hinze (1948))

Modoni et al. (2006) used the theory of Hinze (1948) to express the velocity decay of a submerged jet in the diffusion zone (x<xc), respectively along the longitudinal axis of the jet and in each transverse section, with the following relations

$$\frac{v_{x,r=0}}{v_0} = \Lambda \frac{d_0}{x} \tag{4}$$

$$\frac{v_{x,r}}{v_{x,r=0}} = \frac{1}{[1 + 1 \cdot 33\Lambda^2 (r/x)^2]^2} \tag{5}$$

where r is the distance from the jet axis. By combining Eq. (4) and Eq. (5), the velocity at each point of coordinates (x, r) can be computed as function of the outlet velocity v_0, of the nozzle diameter d_0 and of a dimensionless parameter Λ, which quantifies the interaction between the jet and the surrounding fluid and represents the percentage attenuation of the velocity at a distance of $100*d_0$ from the nozzle.
The hydrodynamic power W of the jet can be computed at any distance x from the nozzle with the following equation:

$$W(x) = \int_0^\infty \rho (v_{x,r})^3 \pi r = \frac{\pi \Lambda \rho d_0^3 v_0^3}{13 \cdot 3x} \tag{6}$$

in which r is the density of the injected fluid (grout for single and double fluid systems, water for triple fluid system). Then, considering the number of nozzles (M) and the residence time (t) of the monitor per unit length L of columns, the lifting speed of the monitor (v_s), the kinetic energy E(x) delivered at a generic distance "x" from the nozzle can be written as

$$W(x) = M \int_{\Delta t} W(x) dt = \frac{\pi M \Lambda \rho d_0^3 v_0^3 L}{13 \cdot 3x v_s} \tag{7}$$

By recalling the expression of the specific energy at the nozzles E'_n, defined as the kinetic energy given at the nozzles per unit length of column (Croce & Flora, 2000)

$$E'_n = \frac{\pi}{8}\frac{M\rho d_0^2 v_0^3}{v_s} \tag{8}$$

And the energy per unit length of column available at a distance x from the nozzle can be obtained from Eq. (7) and Eq. (8) as

$$E'(x) = 0.6\Lambda\frac{d_0}{x}E'_n \tag{9}$$

The problem in using this equation, is that all terms giving the specific energy at the nozzle must be known. Very often, due to how the monitoring instrumentation is arranged, the only known energetic parameter is the so-called specific energy at the pump (Tornaghi, 1989), expressed as

$$E'_p = \frac{pQ}{v_s} \tag{10}$$

in which p is the injection pressure at the pump, Q is the flow rate, and v_s is the average monitor lifting speed. Equations differ because of concentrated and distributed energy losses occurring in the injection circuit. Croce & Flora (2000) pointed out that the difference between Ep' and En' depends on the distance between the pump and the nozzles, but for well-designed facilities and conventional jet grouting technology, energy losses are about 10% of Ep' (Flora & Lirer, 2011; AGI, 2012). Hence, when only Ep' is known, Eq. (10) can be still reasonably applied by assuming the following relation

$$E'_n = 0.9E'_p \tag{11}$$

As far as the interaction between injected and surrounding fluids is concerned, it is convenient to consider explicitly the composition of the eroding fluid (either water or grout) by way of a parameter, Λ^* and to quantify the jet interaction with the surrounding fluid (either grout spoil or air) through a second parameter α (α=1 for single fluid jet grouting where no air wrapping is given, α>1 for double and triple fluid jet grouting). Then, can be written as

$$\Lambda = \alpha\Lambda^* \tag{12}$$

Figure 9 summarizes the values of μ_g and Λ^* for ω (where ω is the water/cement proportion) varying in the interval between 0 (i.e. water without cement) and 2.

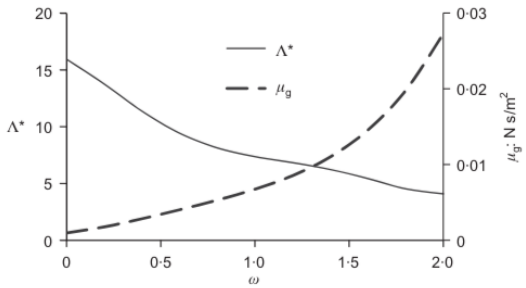

Figure 9 Dependency of Λ∗ on the composition of grout (ρ_c=3000 kg/m3); data for μ_g are taken from Raffle and Greenwood in 1961 (as reported by Bell (1993))

Finally, the diameter will be predicted with the formula

$$D_a = D_{ref} J^{\beta} S^{\delta} \tag{13}$$

Where the adimensional terms J and S represent, respectively, the capacity of erosion of the jet and the soil resistance to erosion. D_{ref} depends of the soil properties and is calibrated alongside the parameters β and δ. The term J in the Eq. (13) stands for the ratio between the specific and a reference kinetic energy.

$$J = \frac{E'(x)}{E'_{ref}(x)} = \frac{\alpha \Lambda^* E'_n}{\alpha_{ref} \Lambda^*_{ref} E'_{n,ref}} \tag{14}$$

In the model formulated by Flora, the refence energy is calculated assuming a monofluid jet grouting with a ratio water/cement ω=1 and a specific kinetic energy at the nozzle of 10 MJ/m. The term S stands for the soil resistance and it is calculated either with the NSPT for granular soils or from the cone tip resistance q_c for cohesive soils with the following equations

$$S = \frac{N_{SPT}}{N_{SPT\,ref}} = \frac{N_{SPT}}{10} \tag{15}$$

$$S = \frac{q_c}{1.5} \tag{16}$$

Substituting the following complete equations are obtained:

$$D_a = D_{ref} \cdot \left(\frac{\alpha \cdot \Lambda^* \cdot E'_n}{7.5 \cdot 10} \right)^{\beta} \cdot \left(\frac{N_{SPT}}{10} \right)^{\delta} \tag{17}$$

$$D_a = D_{ref} \cdot \left(\frac{\alpha \cdot \Lambda^* \cdot E'_n}{7.5 \cdot 10} \right)^{\beta} \cdot \left(\frac{q_c}{1.5} \right)^{\delta} \tag{18}$$

The parameters of the equations to determine the diameter had been calibrated considering experimental data. Three different values of D_{ref} are used depending the soil type and the percentage of fine grains. When both the values of qc and NSPT are given, it can be used the average value obtained for the diameter. All the information about this calculation can be found in the Table 3. Considering that the values that are obtained in some examples collected by the author are the method and the approximations are supposed to be quite correct.

Soil type		ASTM D2487 classification*	D_{ref} : m	β	δ	α, single fluid	α, double and triple fluid
Coarse grained	Without fine	Gravels and sands with less than 5% fines, GW-GP-SW-SP	1·00	0·2	−0·25	1	6
	with fine	Gravels and sands with more than 5% fines, GM-GC-SM-SC	0·80				
Fine grained		Silts, clay and organic soils, CL-ML-OL-CH-MH-OH-Pt	0·50				

*ASTM (2011b).

Table 3 Values of the parameters to be adopted in equations, calibrated on the experimental data collected in the field trials (Flora et al. 2013)

In summary, to predict the column diameter with Flora method the required inputs are the results from SPT and CPTu tests, the pump injection pressure, the W/C relation and the grout flow.

3.3 METHOD 3: SHEN

This third and last method, developed by Shen et al. (2013), like the method of Flora et al. (2013), predicts the jet grouting column diameter based on the theory of the turbulent cinematic fluid and the soil erosion (schematic view shown in Figure 10). This method can be applied to every kind of jet grouting system and, differently from the previous method, includes all the operational parameters, fluid property, soil strength and granulometric distribution, including the effect of injection time on erosion distance.
By giving four examples of jet grouting historical cases tested with this method, the author demonstrates that the diameter can be increased with the use of compressed air (0.5-1.5 MPa) in the bifluid and trifluid systems by a range of 27-81%.

The equation proposed by the author for the diameter of the jet grouting column is:

$$D_0 = 2R_c = 2\eta x_L + D_r \tag{19}$$

Where D_0 is the calculated diameter of the column, R_c the calculated radius of the column, η is the reduction coefficient accounting for the effect of the injection time, x_L is the ultimate erosion distance and D_r is the diameter of the monitor. The monitor diameters usually adopted in the industry are respectively of 60, 76 and 90mm for single fluid, double fluid and triple fluid.

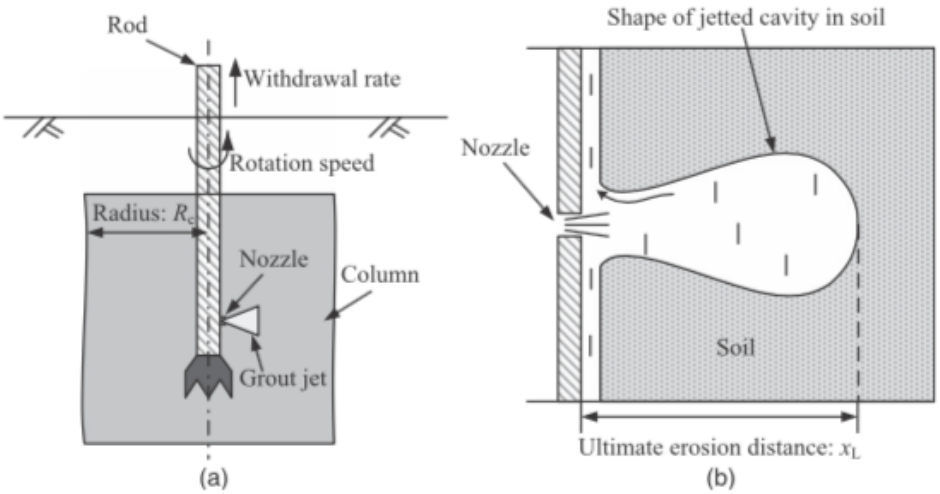

Figure 10 Schematic view of jet grouting (Shen et al. 2013)

In this method the theory of the turbulent kinematic flow has been considered to analyze the distribution of fluid velocity after jetting out from the nozzle (Rajaratnam 1976).

As shown in Figure 11, as fluid with an initial velocity of v_0 is ejected from a round nozzle, two flow regions are developed: (1) initial zone ($x<x_0$) and (2) main zone ($x>x_0$). In the initial zone, the maximum velocity of the jet along the nozzle axis (v_{xmax}) remains constant and is equal to the exit nozzle velocity (v_0).

The influence of the initial zone has been ignored because the range of the initial zone is very limited when the nozzle diameters are very small. Within the main zone, the maximum velocity of the jet along the nozzle axis decreases with distance from the nozzle based on the following relationship (Rajaratnam 1976):

$$\frac{v_{xmax}}{v_0} = \alpha \frac{d_0}{x} \quad (x > x_0) \tag{20}$$

Where v_{xmax} is the maximum velocity of the fluid along the x direction, v_0 is the exit velocity of the fluid at the outlet of the nozzle, d_0 the nozzle diameter and x the distance from the nozzle ($x>x_0$) and alfa the attenuation coefficient, related to the characteristics of the fluid.
The critical velocity v_L is the minimum value of jet velocity that will initiate soil erosion.
If this critical velocity is set equal to the maximum velocity of the fluid along the nozzle axis, the erosion distance x_L can be obtained with the equation:

$$x_L = \frac{\alpha d_0 v_0}{v_L} \tag{21}$$

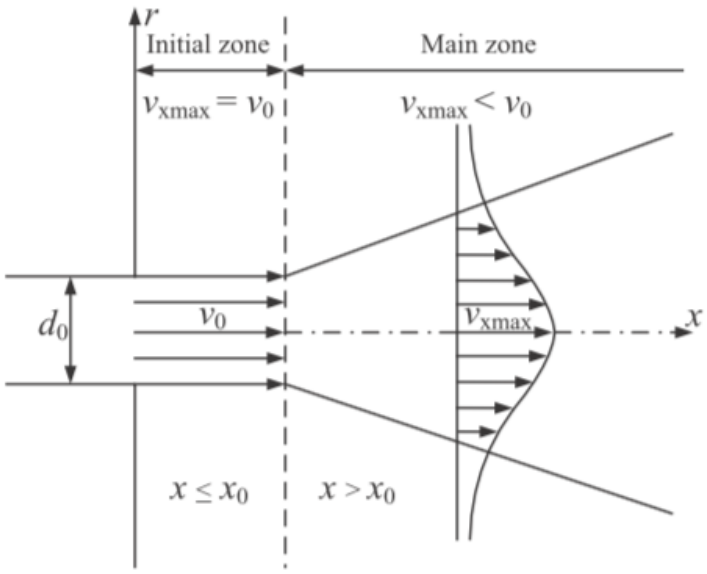

Figure 11 Submerged free jet from a round nozzle (data from Rajaratnam 1976)

The coefficient α describes the degree of attenuation of v_{xmax} with distance x, which formulation is proposed by the author as:

$$\alpha_g = \frac{\alpha_w}{B} \tag{22}$$

Where the parameter α_w has value of 16, proven by different laboratory tests.

The parameter B is expressed as function of the ratio between the laminar kinematic viscosities of grout and water, with the following equation:

$$B = \sqrt{\frac{\mu_g/\rho_g}{\mu_w/\rho_w}} \tag{23}$$

where μ_g= apparent laminar viscosity of grout; μ_w=apparent laminar viscosity of water (0.001 Pa*s); ρ_g=density of grout; and ρ_w=density of water (1,000 kg/m3). To obtain μ_g and ρ_g, the following equations are used

$$\mu_g = 0.007(W/C)^{-2} \tag{24}$$

$$\rho_g = \frac{\rho_w \rho_c [1 + (W/C)]}{\rho_w + \rho_c (W/C)} \tag{25}$$

The value of α differs depending on the system used for the jet grouting:

-For monofluid systems, αs will be the same as the αg, as it is expressed in the equation:

$$\alpha_s = \alpha_g \tag{26}$$

-For bifluid systems, as indicated by Eq. (27),

$$\alpha_d = \varphi \alpha_g \tag{27}$$

With the coefficient ψ given by Eq. (28), where the air pressure compared to the atmospheric pressure is considered

$$\varphi = 1 + 0.054 \frac{p_a}{p_{atm}} \tag{28}$$

-For trifluid systems, at will consider the same parameter ψ, but considering α_w and not αg anymore, as shown in the equation:

$$\alpha_t = \varphi \alpha_w \tag{29}$$

As for the critical velocity, the following equation is considered:

$$v_L = \beta \left(\frac{q_u}{p_{atm}} \right)^k \tag{30}$$

Where q_u is the erosion resistance of soil, p_{atm} is the atmospheric pressure, β is the characteristic velocity when the soil resistance is equal to the atmospheric pressure and k is a dimensionless exponent with a value of 0.5.

The β value is given by the equation:

$$\beta = \begin{cases} b_0 \cdot \left(\frac{M_c}{100} \right)^{b_1} \left(\frac{D_{50}}{D_f} \right)^{b_2}, & 5 \le M_c \le 100 \\ b_0 \cdot \left(\frac{5}{100} \right)^{b_1} \left(\frac{D_{50}}{D_f} \right)^{b_2}, & 0 \le M_c \le 5 \end{cases} \tag{31}$$

Where Mc is the content of fine particles less than 75 μm in size as a percentage, D_{50} is the average size of the soil particle in millimeters and D_f is the size of the No. 200 sieve (0.075 mm).
b_0, b_1 and b_2 are constants with value respectively of 2.87, 0.4 and -0.4.

q_u value only depends of the type of soil (granular or cohesive):

-for cohesive soils

$$q_u = 2C_u \tag{32}$$

Where C_u is the undrained shear strength

-for sandy soils

$$q_u = 2\tau_f \tag{33}$$

Where the τ is the shear strength of sand.

The exit velocity of a fluid jet at the nozzle is related to the flow rate of the injected fluid (Q), nozzle diameter (d_0) and number of nozzles (M). Based on the continuity of flow in the monitor, the exit velocity (v_0) can be obtained as

$$v_0 = \frac{4Q}{M\pi d_0^2} \tag{34}$$

The equation for the reduction coefficient for erosion distance:

$$\eta = a_0 \left(\frac{v_{m0}}{v_m}\right)^{a_1} N^{a_2} \tag{35}$$

Where v_m is the horizontal tangential velocity of the nozzle which is governed by the withdrawal rate v_s and rotation speed of the rod R_s

v_m is given by the equation

$$v_m = \sqrt{(\pi R_s D_r)^2 + v_s^2} \tag{36}$$

where v_m is the horizontal tangential velocity of the nozzle, which is governed by the withdrawal rate v_s and rotation speed of the rod R_s and the diameter of the monitor Dr.

N is the number of passes of the jet, which is determined as follows:

$$N = M\frac{R_s}{v_s}\Delta S_t \tag{37}$$

which is determined by the number of nozzles on the monitor M, the rotation speed Rs, and the withdrawal rate of the rod v_s and the lift step, where ΔS_t is taken as 5 cm in this study, which is a typical value in practice.
a_0 is the correction factor corresponding to the horizontal tangential velocity of the nozzle vm_0 =0.071 m/s, which is calculated based on Rs=15 rpm, vs=30 cm/min, and Dr=90 mm; and a_1 and a_2 as empirical parameters.

In summary, to predict the column diameter with Shen method the required inputs are the pump injection pressure and air pressure, the W/C relation, the soil's granulometry, the grout flow, diameter and number of nozzles, diameter of the monitor, step, time step and rounds per minute during injection.

4 DESCRIPTION OF THE CASE STUDY

4.1 OVERVIEW

The work considered for this study was executed at the port of Rijeka, Croatia, by the Italian company Cos.Idra. The soil treatment was required for the Zagreb Pier Container Terminal in the western part of the Rijeka port, as shown in Figure 12.

Figure 12 zone of field trials in the port of Rijeka (Google Earth)

This project goal is the expansion and modernization of the port to increase its competitiveness (Project Rijeka Gateway II, 2014). The new terminal covers a total area of approx. 17.5 ha (length 680 m, width 210 to 290 m). Part of this area was the existing working port spaces (quays, roads, tracks, warehouses, shelters, installations, power facilities, facilities for employees etc.), with total area of approx. 10.3 ha. The rest of approx. 7.2 ha will be obtained by constructing the new quay and filling the sea. The new quay structure should allow berthing of vessels along a length of 680 m and with depth of 20 m.

The new quay is constructed with reinforced concrete caissons founded on submarine rock embankment. The foundation soil beneath the embankment will be strengthened with gravel column piles and jet grouting.

General level of the quay (quay zone wide approximately 40 m) is +4.05 m. This is a zone for ship berthing and gantry crane operation (track spacing 35 m).

Figure 13 and 14 show, respectively, the key plan of the project and a partial section of it.

Apron and stacking area will be arranged by filling up stone material in the area behind the quay structure to the project border, i.e. to the shunt tracks in the north. Stacking area with associated roads is long 680 m and wide from 170 to 250 m.

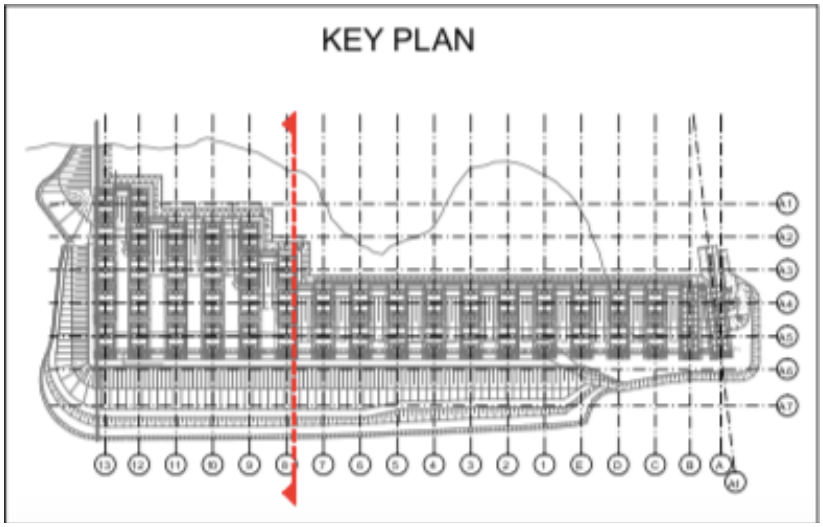

Figure 13 zone used for field trials (Report RGP Book 2-Volume 3)

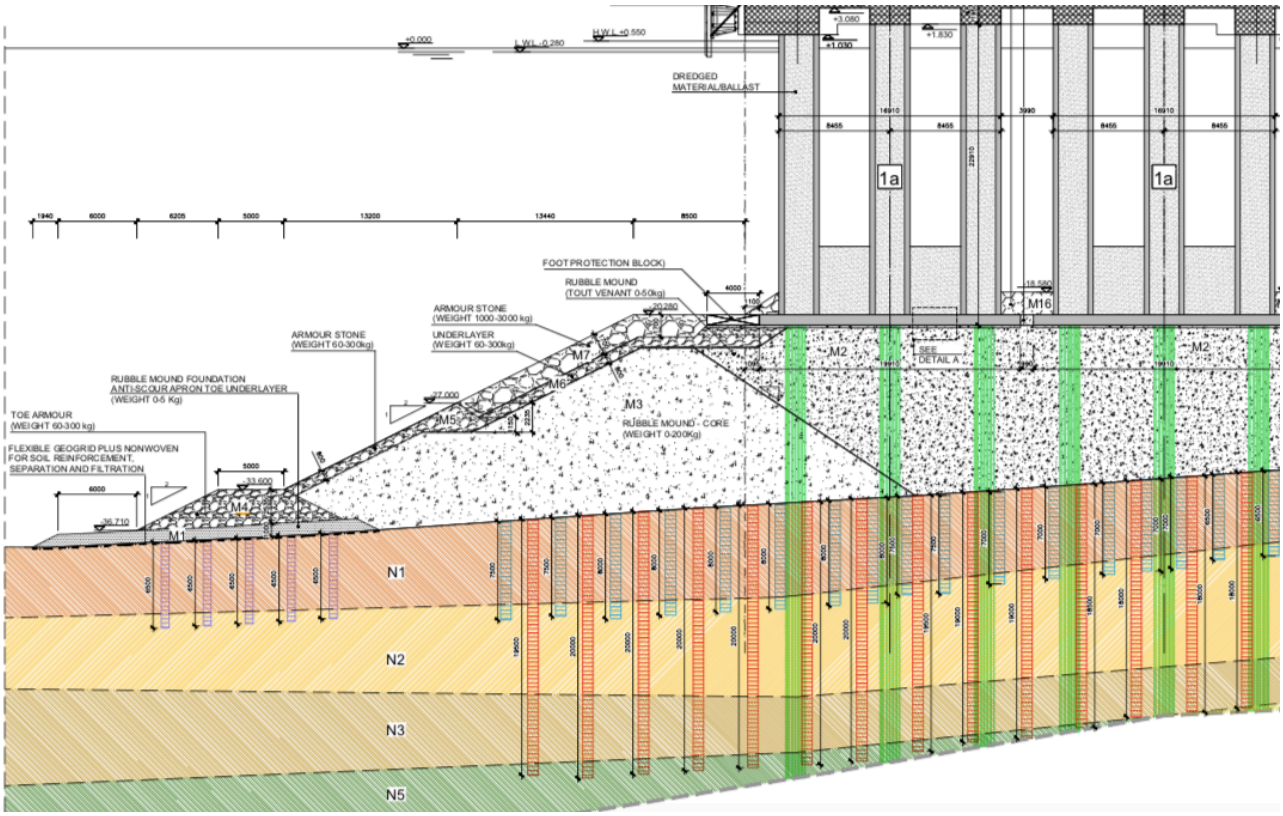

Figure 14 Typical cross section (Report RGP Book 2-Volume 3)

4.2 GEOTECHNICAL CONDITIONS

4.2.1 GROUND UNITS

Soil types divider per layer are shown in Table 4 and Figure 15.
The rubble mound is Layer N0 is stone deposit, consisting of debris, rock debris and blocks of stone, heterogeneous composition, mixed with sandy silty clay, and the surface of the waste building materials.

Layer N5 (sandy clayey medium gravel dense to very dense) is not reported in the table because is not crossed by the jet grouting column.

LAYER	MATERIAL TYPE	LAYER THICKNESS	AGE
WATER	/	16.15 m	/
N0	Rubble mound	15 m	Recent
N1	Very soft silty sandy clay	17 m	Quaternary period
N2	Clayey silty fine to medium carbonaceous sand	1.5 m	Quaternary period
N3	Very soft to soft silty clay	4 m	Quaternary period
N4	Clayey sand	0.1 m	Quaternary period
ROCK	Limestone and carbonate mudstone	2 m	Lower cretaceous period

Table 4 soil types divided per layer

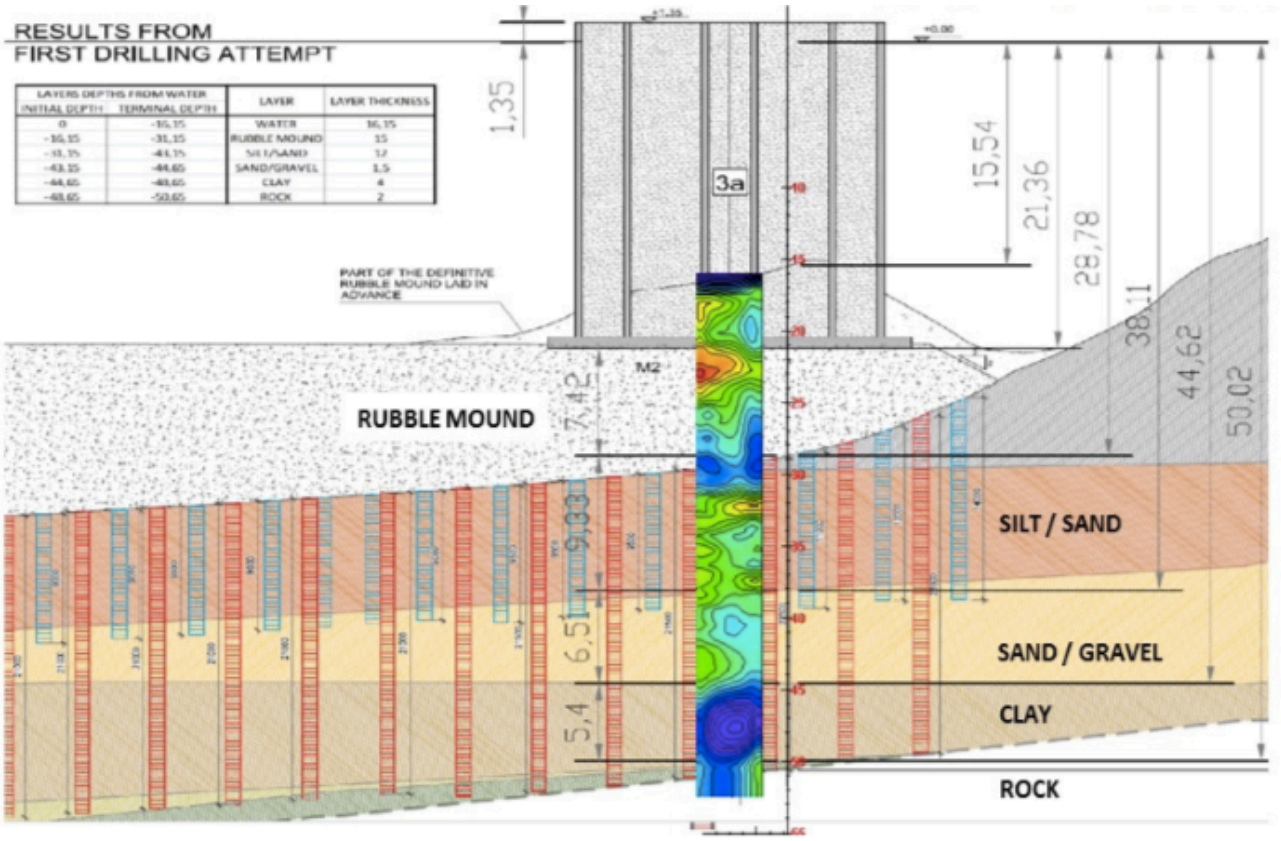

Figure 15 scheme of a jet grouting column in the field trial (Report RGP Book 2-Volume 3)

4.2.2 GEOTECHNICAL PROPERTIES

Table 5 shows the different soil parameters for each layer considered for the zone of field trials.

PHASE 1 - 0C							
IDENTIFICATION		CHARACTERISTICS					
Level	Description	Unit weight	Angle of internal friction	Cohesion	Young's Modulus	undrained cohesion	Oedometer modulus
		γ	φ	c'	E	c_u	E_{ed}
[n°]		[kN/m^3]	[°]	[kPa]	[kPa]	[kPa]	[kPa]
N-0	Madeground	20	35	-	30000	-	-
N-1	Clay	19	22	-	-	2xZ	4000-6000
N-2	Sand	20	30-35	-	15000	-	-
N-3	Clay	19	25	-	-	2xZ	6000-8000
N-4	Dense sand	20	33-35	-	15000-20000	-	-
N-5	Gravel	20	40-42	-	30000-40000	-	-
N-6	Limestone/mudstone	25	35	100	100000	-	-

Table 5 Soil geotechnical parameters (Report RGP Book 2-Volume 3)

Figure 16 shows the values of water pressure (u), effective (σ'z) and total stresses (σz) varying with depth.
While water pressure line increases directly proportional, total and effective stress lines vary their slope at the beginning of N0 (23m) and then increase almost constantly.

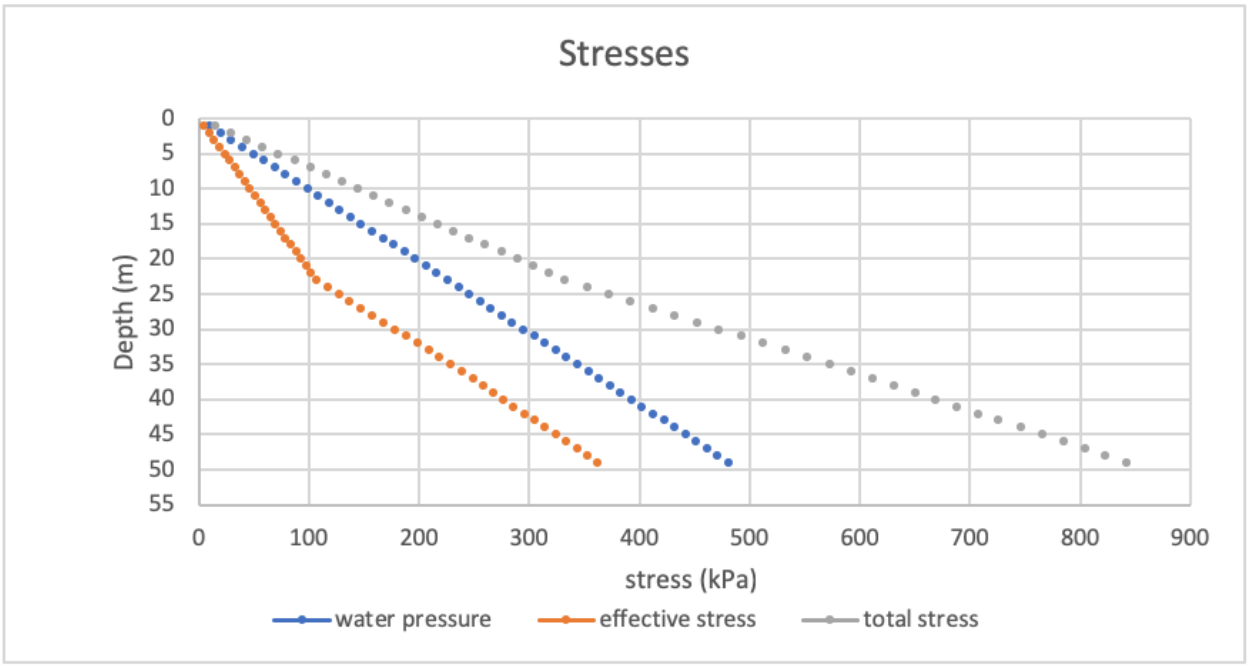

Figure 16 u, σz, σ'z in the field trial

The soil layers that are more critical compared to the foundation's stability are the N1, N2 and N3. These layers reach a depth of 30m below the seabed and have been investigated in laboratory with CPTu (Figure 17) and SPT tests (Figure 18), giving the following results.

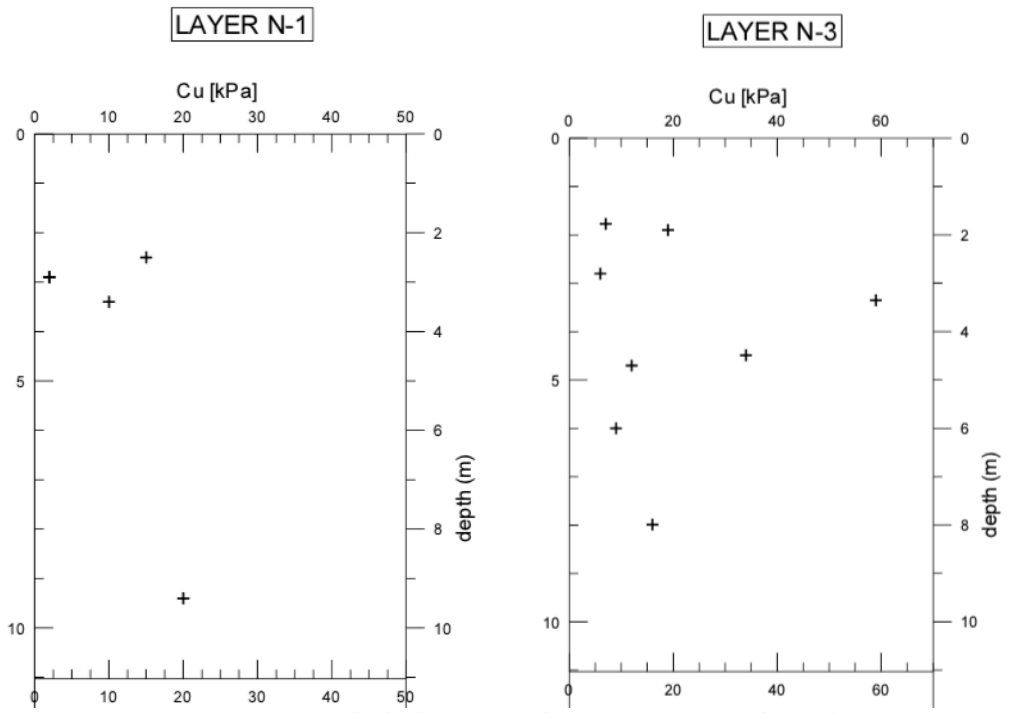

Figure 17 CPTu test results for layers N1 and N3 (Report RGP Book 2-Volume 2)

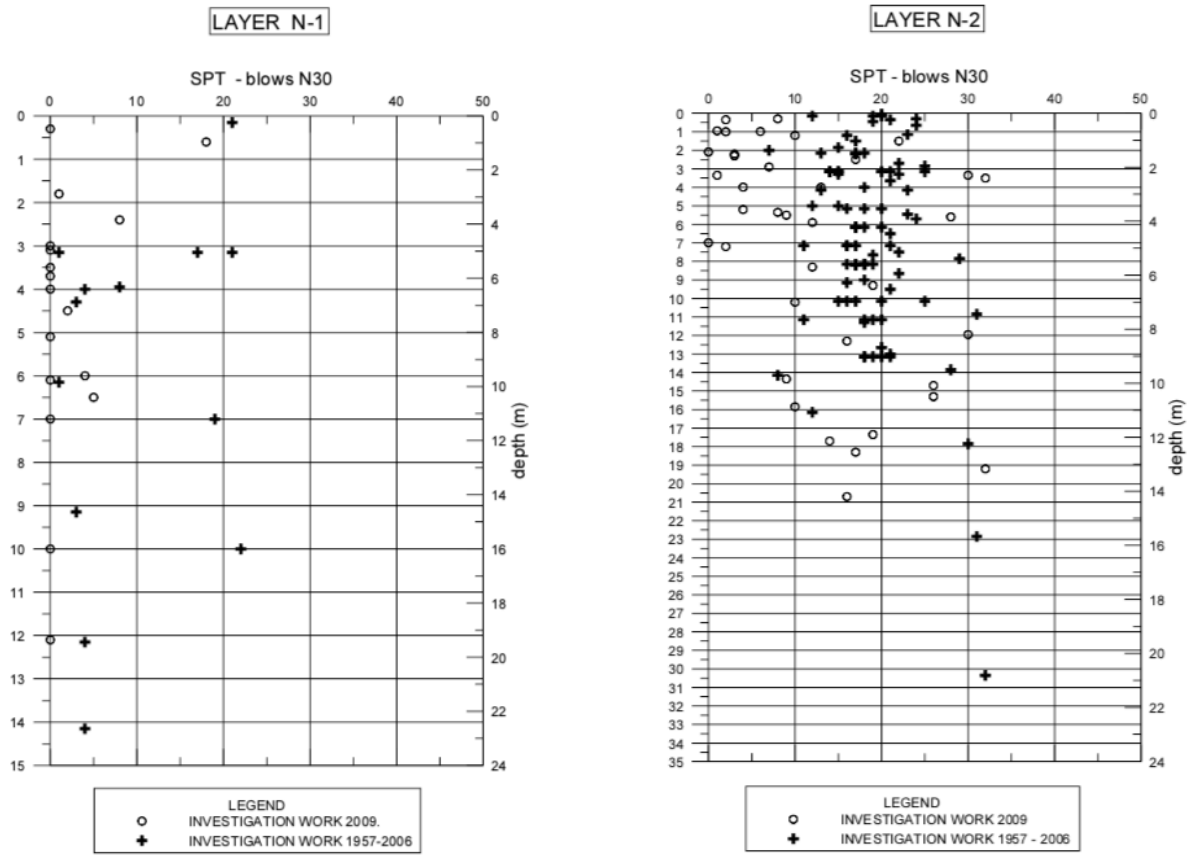

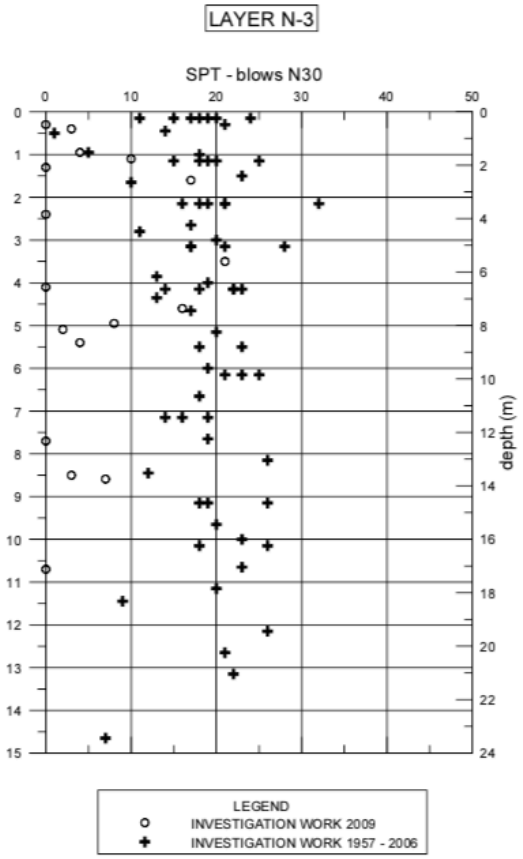

Figure 18 SPT test results for layers N1, N2, N3 (Report RGP Book 2-Volume 2)

The value of resistance obtained is:

$$q_c\ (MPa) = 0.048z\ (m) \tag{38}$$

Assuming the unit weight of soil is γ=20 (kN/m^3), the buoyant weight of soil is γb=10 (kN/m^3), the vertical stress and effective stress in soil (adjusted for water depth) are given by σv_0 (MPa)=0.02 z (m) and $\sigma v'_0$ (MPa) =0.01 z (m). Using the usual relationship (Robertson, 2009) with N_k=14, a general value of Cu is obtained for all the layers:

$$C_u\ (kPa) = 2z\ (m) \tag{39}$$

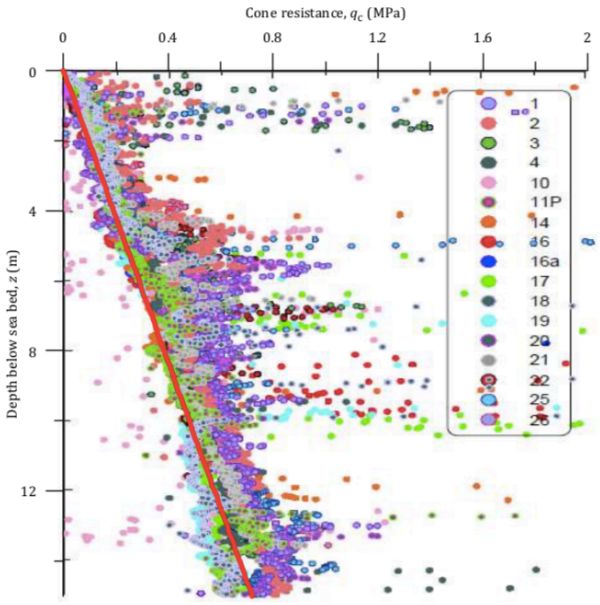

Figure 19 Stage 1 CPT data (Lankelma, as reported by GCG-UK 2010, Fig. 11.1.3) qc (MPa) = 0.048z (m)

It is to be emphasized that the depth refers to the depth below the seabed, which needs not to be horizontal, and not to the absolute depth (plot shown in Figure 19).

Figures 20 show the different fine percentage for every layer.

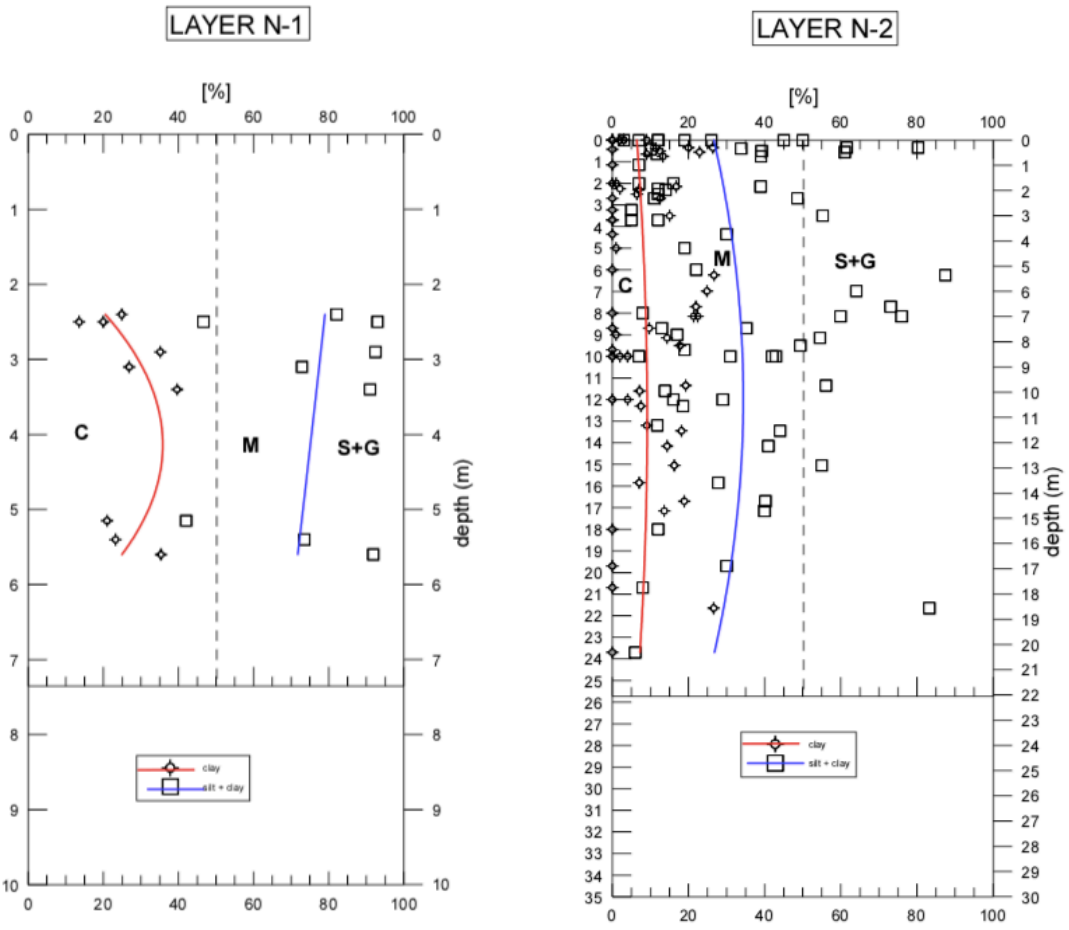

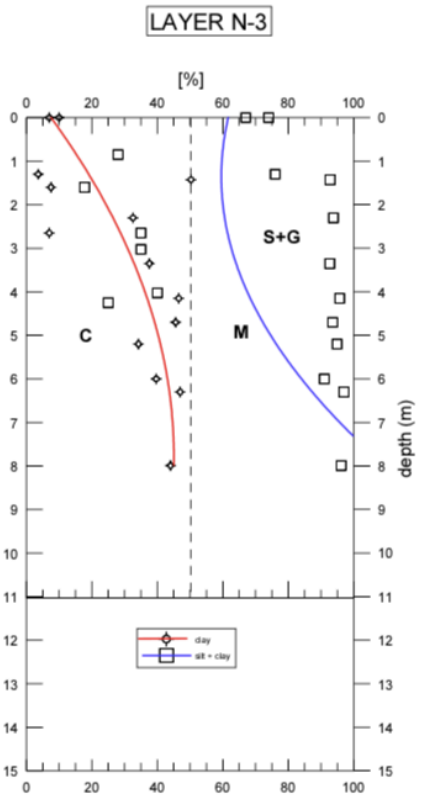

Figure 20 fine percentage for layers N1, N2, N3 (Report RGP Book 2-Volume 2)

4.3 JET GROUTING TREATMENT

4.3.1 MOTIVATION AND LAYOUT

The jet grouting columns are part of the scheme of construction, which is divided as follows (Report RGP 2-3):

- Stone columns performance and geogrid installation;
- Rubble mound execution to the level -21.08 m a.s.l.;
- Preload of the rubble mound;
- Preload removing after consolidation of the foundation soil;
- Caissons installation;
- Performance of jet grouted columns below caissons;
- Upper deck performance;
- Placing of coarse fill behind the inland facing caisson

Jet grouting is performed after installation of caissons. Required diameters of jet grouting are 1400 and 1700mm, length from the limestone rock to the caisson's foundation slab at 21.08 m a.s.l. Under each caisson, 9 jet grouted columns will be performed - 3 units of 1400mm diameter and 6 units of 1700mm diameter. They will be performed with raster 7.2x4.75m.

Jet grouted columns are designed to transfer the vertical live loads from the upper deck (STS crane rail, containers) to the base rock. This avoids additional settlement due to the live loads in the exploitation phase.

In a numerical soil-structure interaction analysis the verification of stability with regard to the ultimate limit state can be calculated using the phi/c reduction technique implemented in the Plaxis 2D program. This analysis starts from an equilibrium state of the structure already loaded by unfavorable design loads by gradually reducing soil strength parameters by a factor. If the value of this factor is larger or equal to the required material factor of Eurocode 7 and the structure is still in equilibrium, the stability for the ultimate limit state is assumed to be verified. In the study (Report RGP Book 2-Volume 2) it is demonstrated that jet grouting columns improve global stability.

After jet grouted column construction, the upper deck will be cast in place. After the deck, behind the inland facing caisson a coarse fill is placed. This last sequence marks the end of main construction sequences of the pier structure.

Figure 21 shows the complete planimetry of the port with the 49 caissons involved.

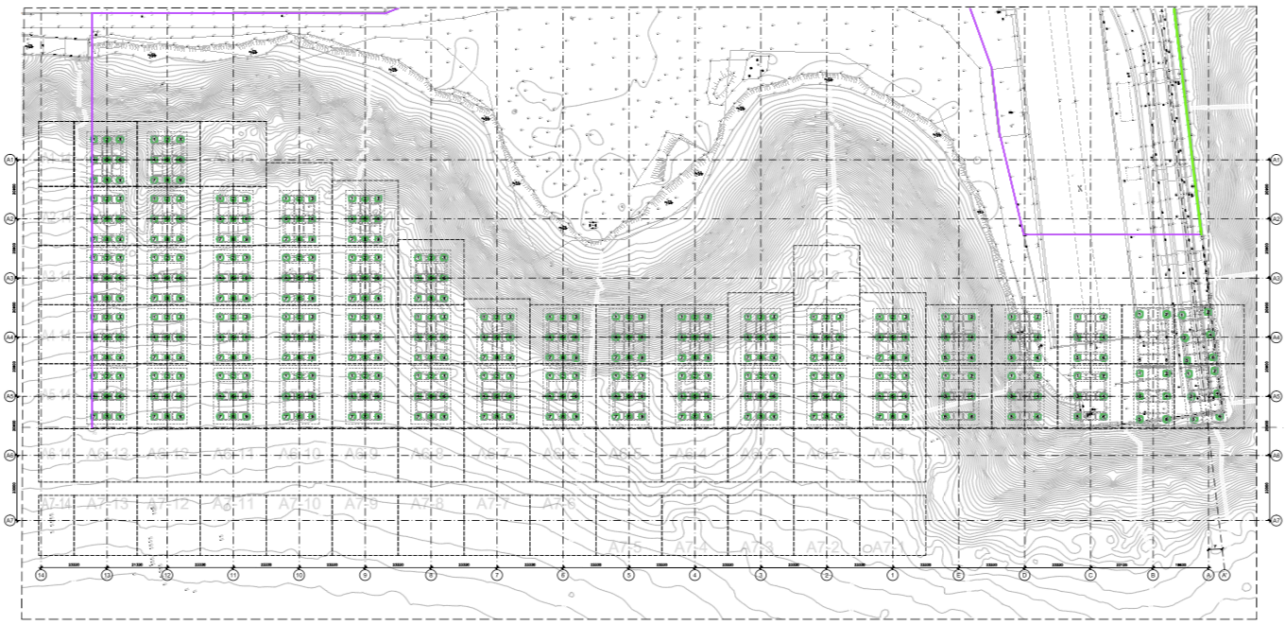

Figure 21 the 49 caissons position in the project (Report RGP Book 2-Volume 3)

the specific weight of the caisson placed on top of the rubble mound can be found in (Report RGP Book 2-Volume3) where the parameters of the caisson used for the field trials (caisson type 3) are as shown in Table 6:

CASSION TYPE 3 (C3)

CAISSON 3 (design)	B (m)	L (m)	A (m^2)	h (m)	V (m^3)	γ (kN/m^3)	G (kN)
deck_0 (concrete)	14,00	19,91	278,74	0,80	222,99	24,00	5351,81
walls_1 (concrete)	-	-	36,72	22,07	810,41	24,00	19449,85
walls_2 (concrete)	-	-	12,57	22,07	277,42	24,00	6658,08
fill_1 (rock material)	-	-	63,45	22,07	1400,34	18,00	25206,15
fill_2 (rock material)	-	-	73,27	22,07	1617,07	18,00	29107,24
					V_{C3}= 4328,23		G_{C3}= 85773,12

CAISSON 3 (model)	B_m (m)	L_m (m)	h_m (m)	V_m (m^2)	G_m (kN)	$G_m/V_m = \gamma_m$ (kN/m^3)
caisson (cocrete+fill)	14,00	16,90	25,13	5945,76	85773,12	14,43

CAISSON 3 (model/m')	B_m (m)	d (m)	B_m/d	γ_m (kN/m^3)	γ_m (kN/m^3/m')
caisson per meter	*14,00*	*23,33*	*0,60*	*14,43*	*8,66*

Table 6 parameters for caisson type 3 (Report RGP Book 2-Volume 3)

Meanwhile caisson's geometry is shown in Figure 22:

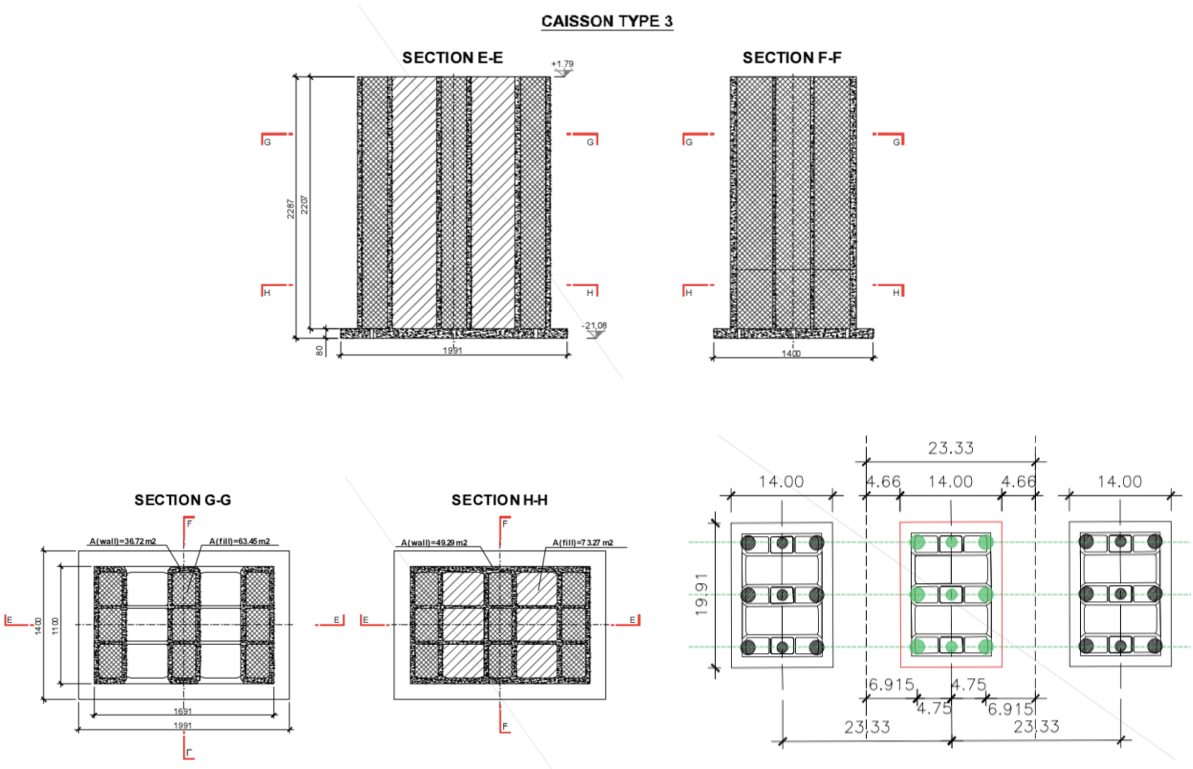

Figure 22 caisson type 3 dimensions (Report RGP Book 2-Volume 3)

4.3.2 MONITORING DURING EXECUTION

For the jet grouting column execution, the control device from the Company Jean Lutz (http://www.jeanlutzsa.fr/en/about/) is used. Through its monitoring system it controls the following parameters during the perforation and the injection: lifting rate, rotation, grout pressure, grout flow, volume by meter, station time, air flow and air pressure (for the bifluid and trifluid system), as it can be seen in Figure 23.

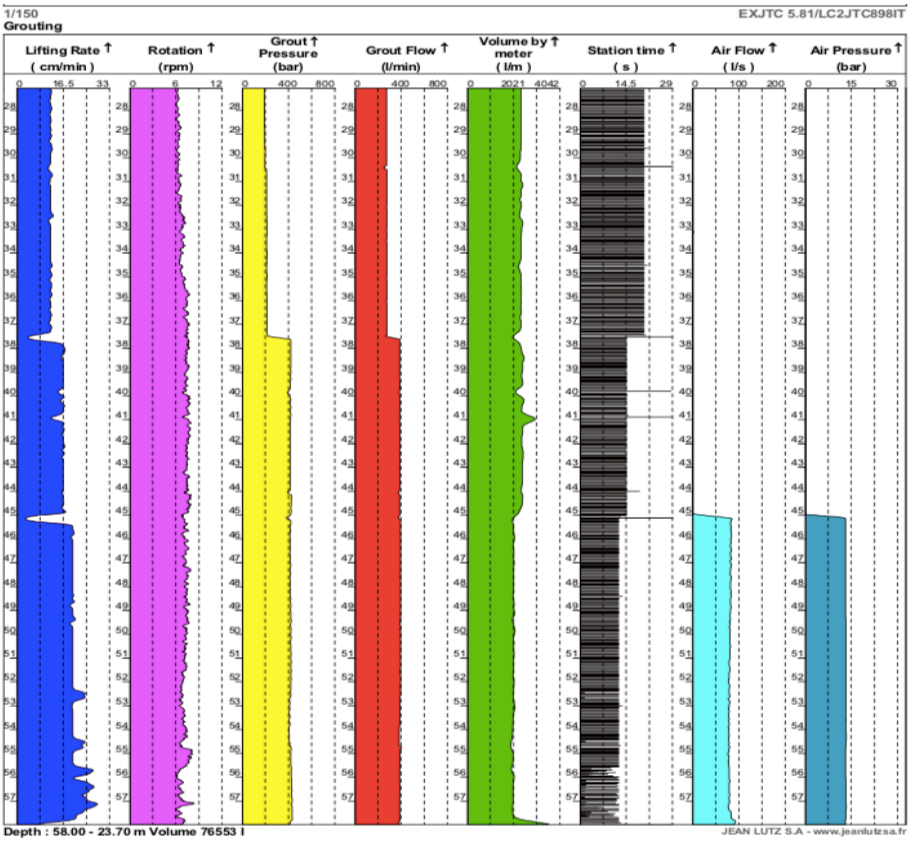

Figure 23 values measured with Jean Lutz instrumentation during injection

Table 7 shows all the input parameters involved in the execution of the column: Grout pressure, grout flow, lifting speed, time step, air pressure, the number of nozzles, the lifting step and the rounds per minute.

CAISSON	COLUMN	SYSTEM	FLUID	MIX	PRESSURE	L/min	Inc. from Vert.	N./Ø NOZZLES
	1	BIFLUIDO	Grout	☒ 2 ☐	>400 bar	426	0 °	1 / 6,5
			Air		16 bar	13000		
		Q.ty 1: 30,58	U.W.: 1,51	reading time: 14:45		ROUNDS/min 7		
		STEP cm: 5	STEP sec: 9,10	NOTES:				
	1	BIFLUIDO	Grout	☒ 2 ☐	>400 bar	426	0 °	1 / 6,5
			Air		16 bar	13000		
		Q.ty 1: 34,36	U.W.: 1,52	reading time: 14:20		ROUNDS/min 7		
		STEP cm: 5	STEP sec: 9,10	NOTES:				
	1	BIFLUIDO	Grout	☒ 2 ☐	>400 bar	426	0 °	1 / 6,5
			Air		16 bar	13000		
		Q.ty 1: 44,65	U.W.: 1,50	reading time: 12:10		ROUNDS/min 7		
		STEP cm: 5	STEP sec: 9,10	NOTES:				

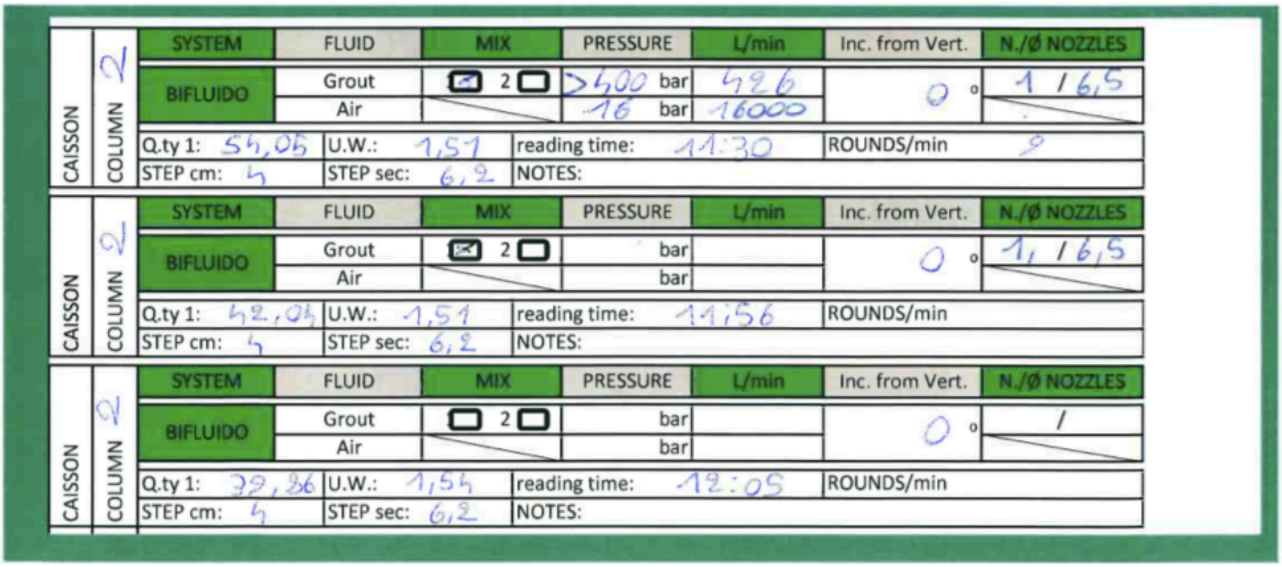

CAISSON	COLUMN	SYSTEM	FLUID	MIX	PRESSURE	L/min	Inc. from Vert.	N./Ø NOZZLES
	1	BIFLUIDO	Grout	☒ 2 ☐	>400 bar	428	0 °	1 / 6,5
			Air		16 bar	16000		
		Q.ty 1: 54,05	U.W.: 1,51	reading time: 11:30			ROUNDS/min 9	
		STEP cm: 4	STEP sec: 6,2	NOTES:				
	2	BIFLUIDO	Grout	☒ 2 ☐	bar		0 °	1, / 6,5
			Air		bar			
		Q.ty 1: 42,04	U.W.: 1,51	reading time: 11:56			ROUNDS/min	
		STEP cm: 4	STEP sec: 6,2	NOTES:				
	3	BIFLUIDO	Grout	☐ 2 ☐	bar		0 °	/
			Air		bar			
		Q.ty 1: 39,86	U.W.: 1,54	reading time: 12:05			ROUNDS/min	
		STEP cm: 4	STEP sec: 6,2	NOTES:				

Table 7 parameters of injection

4.4 QUALITY CONTROLS

Due to the marked variability of the geotechnical properties of the subsoil layers, a test site (Report Rijeka Harbor by Geostudi Astier, 2016) was planned to design the proper jetting and drilling settings of the treatment.

The test site area is located below the first caisson row: six jet columns were performed with different drilling and injection parameters (as shown in Table 8) and then submitted to both geophysical monitoring and core sampling, in order to assess the effectiveness of the injections. Figure 24 shows the geometry and position of the wells used for electrical resistivity and seismic surveys (BH1-2-3-4-5-6) and the position of the jet columns (C1-2-3-4-5-6). Geophysical boreholes are around 3.5-4.0 meters distant and they were designed so that the 6 jet columns could be suitably imaged by ERT and seismic methods, in order to derive the mechanical properties of the treated soil.

	P (kPa)	Q (m^3/s)	Vs (m/s)	ΔT (s)	Pa (kPa)	N NOZZLES	STEP (cm)	RPM
COLUMN 1	40000	0.0071	0.004	9.1	1600	1	4	7
COLUMN 2			0.006	6.2				9
COLUMN 3			0.007	5.8				8
COLUMN 4			0.006	6.5				8
COLUMN 5			0.004	10.2				6.5
COLUMN 6			0.004	11.2				6.5

Table 8 injection instrumentation input parameters

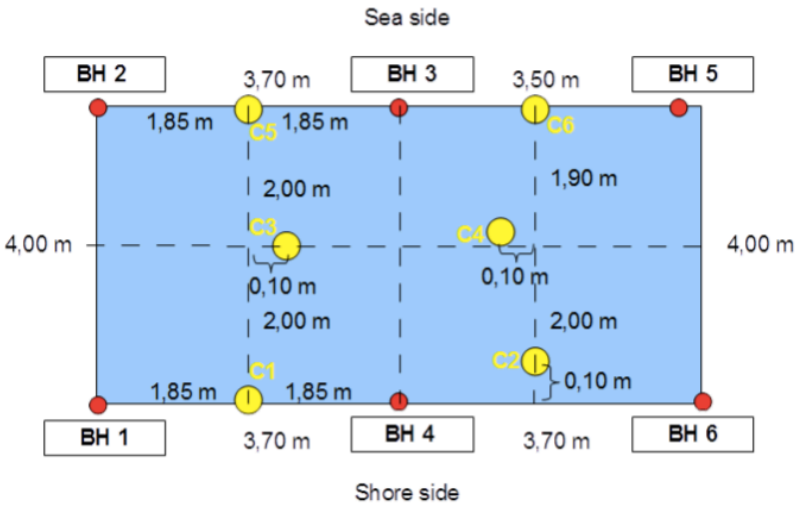

Figure 24 position of boreholes and jet columns (Report Rijeka Harbor by Geostudi Astier, 2016)

A description of the two quality control methods of cross-hole electric resistivity tomography (ERT) and seismic tomography is given, which estimate the columns diameter and the continuity of injection.

4.4.1 CROSS-HOLE ERT METHOD

Electrical resistivity tomography (ERT) is a geophysical technique designed to locate and measure changes in the electrical resistivity of the subsurface. The electrical resistivity of the ground is due to a combination of lithology, structures, weathering and pore water. Resistivity can be influenced by several factors including different soil types, grain size, clay minerals content (Report Rijeka Harbor by Geostudi Astier, 2016).

Cross-hole Electrical Resistivity Tomography is a specific application of ERT that makes use of electrodes installed inside boreholes while usually those are laid out on the terrain surface.

A single ERT data point requires a four electrodes resistance measurement (quadrupole scheme): two electrodes to inject current and two other electrodes to measure the resulting potential. In general tomography requires addressing tens of electrodes and making hundreds or thousands of such measurements in a timely and optimized fashion. The resistivity of the subsurface is then calculated from these data points using an inversion algorithm, so that the geology can be interpreted from the overall volume of results.

The optimal combination of measurements (set of quadrupoles) was determined after a series of preliminary tests over the entire set of boreholes, during the pre-injection survey and then applied to the post-injection survey too, to ensure homogeneity and reliability of the method. Two array styles were used: Dipole-Dipole and Pole-Dipole as these complement each other and are a useful check on the results. In the pole-dipole array, one current electrode (transmitter) is located on the surface some distance away from the potential electrodes (receivers), as shown in Figure 25. The pole-dipole measurements were set up so that the current and potential electrodes were not in the same borehole so that borehole effects were minimized.

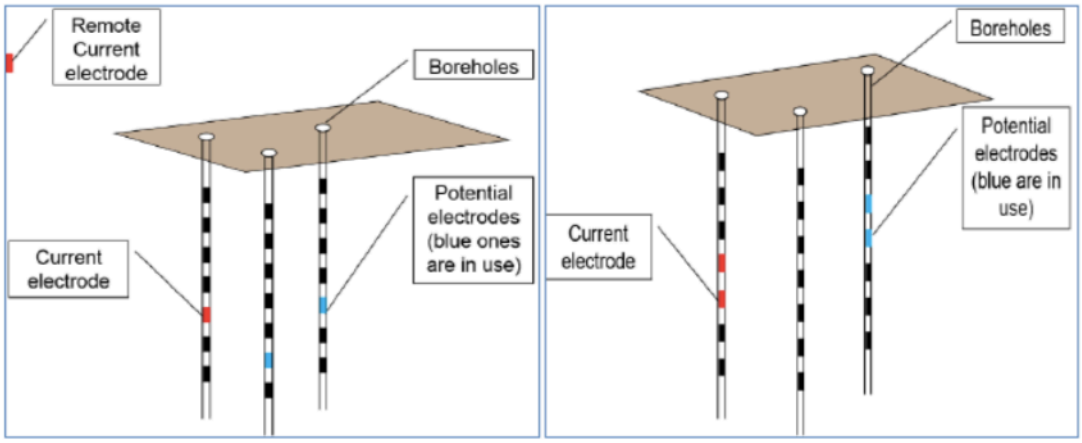

Figure 25 Configuration of Cross-hole Electrical Resistivity a) Pole-Dipole array b) Dipole-Dipole array (Report Rijeka Harbor by Geostudi Astier, 2016)

Generally speaking, the electrical resistivity of soils and sediments is a factor of:

- water saturation
- clay content (presence of silts and clays reduces soil resistivity)
- effective soil porosity
- salinity of the fluid filling the pores
- temperature
- presence of organic matters like peat, hydrocarbons, solvents, etc.
- grain size and granular composition
- insulating matters: the injection into the ground of fluids with high insulating characteristics like water/cement grouts or resins causes a noticeable increase of resistivity due to the elimination of the pore spaces needed for the flow of electric current.

The hydration and curing of cement-based grouts does affect the overall resistivity of the soil subject to injection, due to interconnections between soil grains established by the grouting and to the elimination/displacement of water (except of that strictly needed for hydration). The result is the production of a solidified soil matrix called “soilcrete”, initially liquid, then plastic and finally solid.

For the ERT surveys two resistivity models are available:
➢the one derived from resistivity measurements BEFORE treatment, that is also useful in

describing the general lithology, and
➢the model AFTER the injections which describes how the background resistivity of the initial

model has been changed by the grout treatment.

Usually the visualization of post-treatment resistivity models is performed through the calculation of the PERCENTAGE DIFFERENCE RESISTIVITY MODEL, built on the basis of the following function:

% Resistivity Variation = 100 x (Resistivity_POST- Resistivity_PRE)/Resistivity_PRE

Positive variations (usually addressed in the colourmaps with yellow-red colors) indicate a resistivity increment: we expect such a behavior for grout saturating the sediment pores and hence when the jet column is correctly generated. Negative variations (cyan-blue color) show a decrease of resistivity after treatment and could be associated to a limited effectiveness of the treatment. (example shown in Figure 26).

Changes of percentile soil resistivity of a supposedly injected soil mass will indicate if total or partial soil modification (jet grouting column formation in our case) has been achieved. For instance, the consequence of using inadequate jetting procedures may be a significant (and useless) dispersion of grout (often due to excessive jetting pressure) that ERT would evidence as low resistivity readings in zones of otherwise expected high cement concentration and scattered high resistivity readings in zones of cement dispersion.

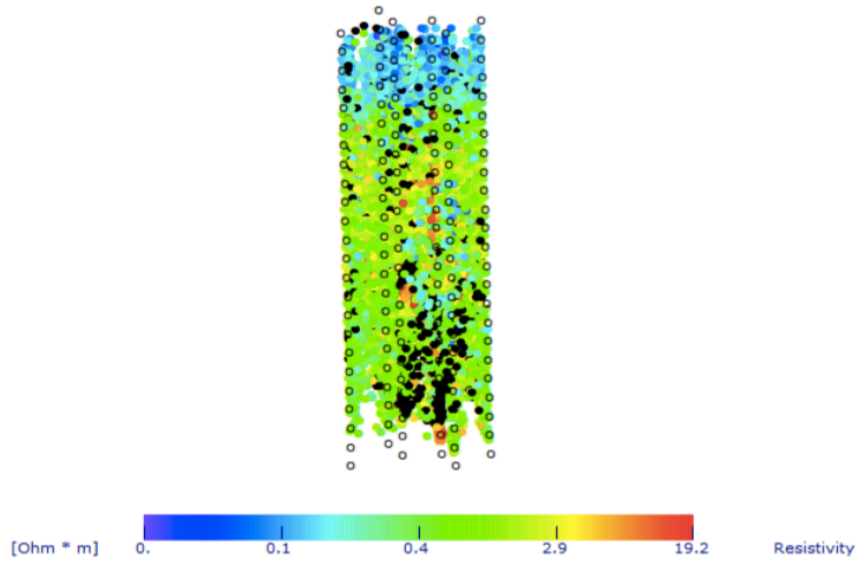

Figure 26 Results example for an ERT test (Report Rijeka Harbor by Geostudi Astier, 2016)

4.4.2 CROSS-HOLE SEISMIC METHOD

The sonic tomography method derives the distribution of sonic velocity on 2D sections of the object under investigation (Report Rijeka Harbor by Geostudi Astier, 2016).

Cross-hole measurements are based on the analysis of the elastic impulses generated inside a borehole by an energy source and received in a second borehole after passing through the investigated media (see Figure 27). The propagation mode of the elastic wave is strictly dependent on the elastic properties and structure of the material. The elastic waves are received by specific sensors which convert them in form of electric signals.

The main issue in the velocity analysis is the estimation of travel times and distances. Velocities (V) of the material between source and receiver points are computed by means of a time (t) to distance (d) inversion.

$$V = d/t \tag{40}$$

Compressional and shear wave velocities are calculated using travel times once the distance between generation and receiving points is known. For this purpose, the verticality of each borehole is needed.

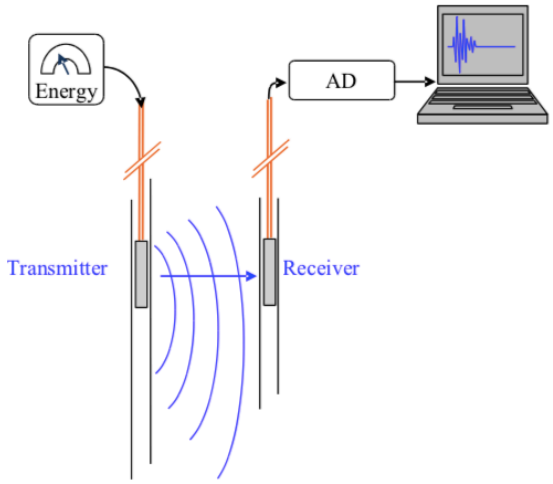

Figure 27 sonic cross-hole method scheme (Report Rijeka Harbor by Geostudi Astier, 2016)

For the determination of the velocity field in the investigated sections, the software TOMOELAB developed by ISMES is used. This software, starting from an initial sonic velocity model, iteratively reconstructs the velocity field with a numerical procedure S.I.R.T. (Simultaneous Iterative Reconstruction Technique), gradually reducing the gap between the times measured along the different paths and the calculated times, the latter obtained by considering the model of the velocity field determined at each iteration. (Figure 28)

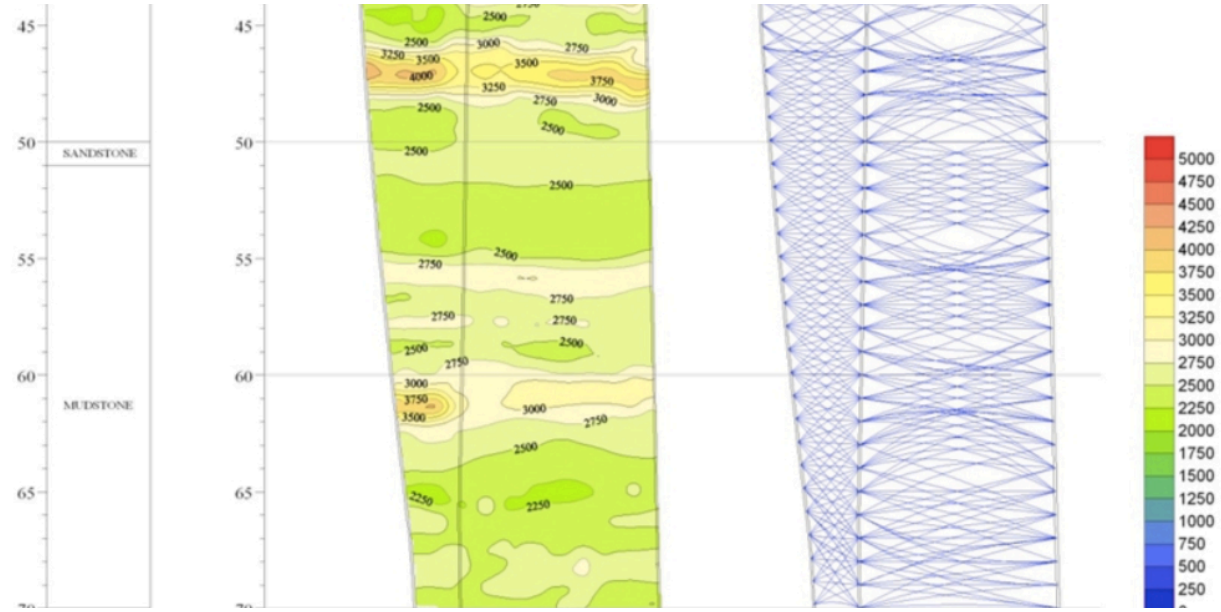

Figure 28 Example of Cross-Hole ray-path network and related interpretation (Report Rijeka Harbor by Geostudi Astier, 2016)

Cross-hole seismic measurements, instead, were performed only after the grouting as it is usually very difficult to maintain the same conditions of the installed (and cemented) pipes, and to ensure a proper comparison. In fact, even in this case, proper installation of PVC pipes has been repeated after grouting because some of the previously installed ones were damaged by the high-pressure injections. ERT cables do not suffer from this problem so they can resist and be used for both background and post-injection measurements.

Seismic velocities in marine sediments are clearly constrained by water velocity Vp, around 1500 m/s. So usually the average of Vp velocities (Table 9) in natural sediments is below 1900 m/s with higher values related to higher density and coarser grain size (1800-1900 m/s) and lower velocities associated to clayey-silty layers (1500-1600 m/s). The effect of grout saturating the pores turns into an increment of these velocities above 2000 m/s or more.

TABLE 1. Sediment Properties, Continental Terrace (Shelf and Slope) Environment

Sediment Type	No. Samples	Grain Diameter Mean, mm	Grain Diameter Median, mm	Sand, %	Silt, %	Clay, %	Bulk Grain Density, g/cc	Density, g/cc Avg.	Density, g/cc SE	Porosity, % Avg.	Porosity, % SE	Velocity, m/sec Avg.	Velocity, m/sec SE	Ratio Avg.	Ratio SE
Sand															
Coarse	2	0.530	0.520	100.0	...	...	2.71	2.03	...	38.6	...	1836	...	1.201	...
Fine	9	0.153	0.171	88.1	6.3	7.1	2.70	1.98	0.024	43.9	1 29	1742	10	1.139	0.006
Very fine	3	0.090	0.094	83.9	13.0	2 9	2.74	1.91	...	47.4	...	1711	...	1.121	...
Silty sand	11	0 073	0.126	65 0	21.6	13.4	2.71	1.83	0.025	52.8	1.55	1677	9	1 096	0 006
Sandy silt	6	0.036	0.051	34.5	51.2	14.3	2.75	1.56	...	68.3	...	1552	...	1.015	...
Sand-silt-clay	17	0.018	0.041	32.6	41.2	26.1	2.71	1.58	0.030	67.5	1.66	1578	9	1.032	0.006
Clayey silt	40	0.006	0.011	6 1	59.2	34.8	2.71*	1.43	0.016	75.0	0.87	1535	3	1.004	0.002
Silty clay	17	0.003	0.004	5.3	41.5	53.6	2.69	1.42	0.013	76.0	0.74	1519	3	0.994	0.002

Notes.

Laboratory values: 23°C, 1 atm; density, saturated bulk density; porosity, salt free; ratio, velocity in sediment/velocity in seawater at 23°C, 1 atm, and salinity of sediment pore water.

SE: Standard error of the mean.

* Five samples.

EDWIN L. HAMILTON

Table 9 Sediment properties (Report Rijeka Harbor by Geostudi Astier, 2016)

4.4.3 RESULTS

Results for both ERT and seismic cross-hole tests described by Geostudi Astier (2016) are summarized as follows. ERT results are shown in function of % difference of electrical resistivity (before and after the treatment), meanwhile seismic results are in function of P-waves velocity.

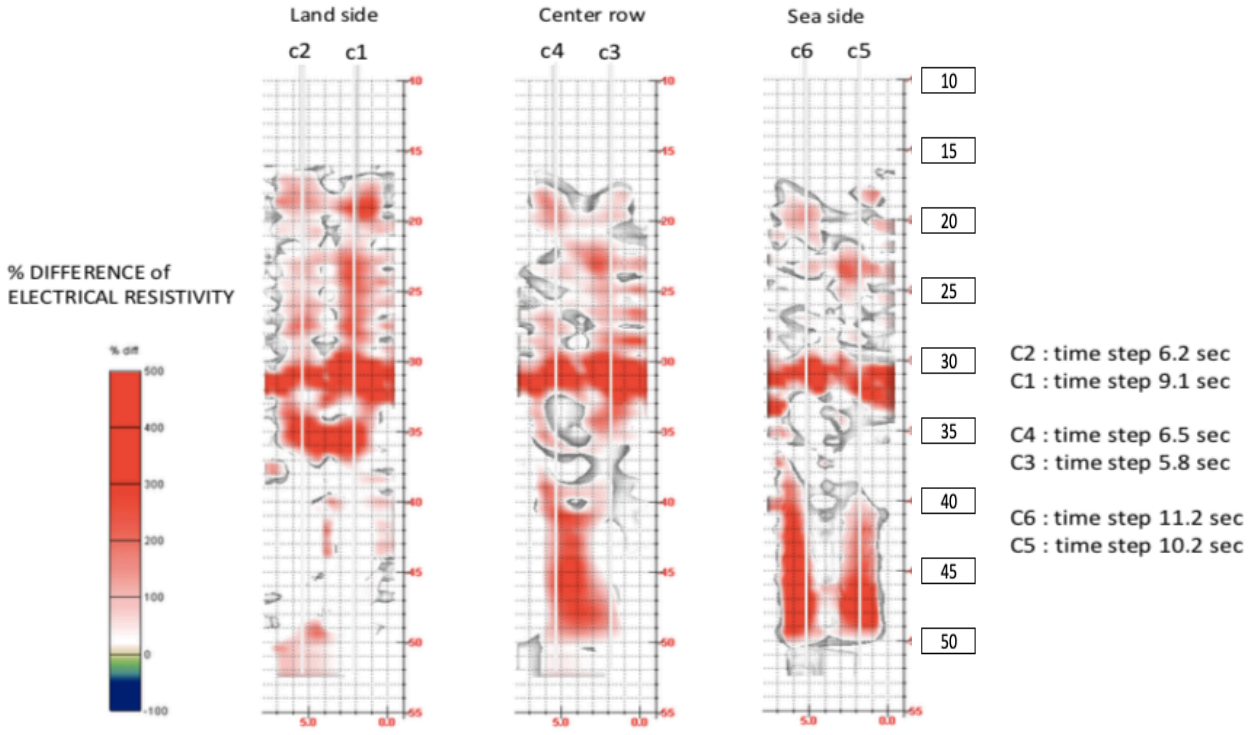

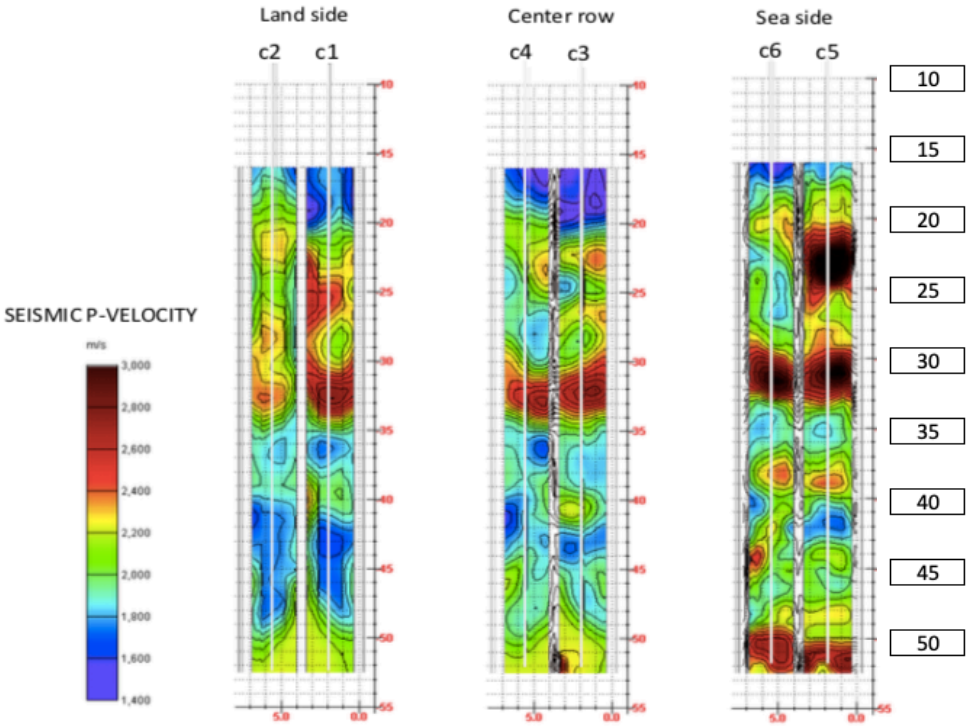

Figure 29 summary of % resistivity difference (above) and seismic P velocity sections (below) (Report Rijeka Harbor by Geostudi Astier, 2016)

The geophysical data collected (results summarized below in Figure 29, where the percent resistivity variation is showing only the values higher than 20%) and the successive integration with drilling, coring and laboratory measurements allow to conclude that:

- the sediments modified by jet grouting show very significant variations of electrical properties in parts of the volume investigated (fig. 29), with marked increases of resistivity (well above 100% in many portions, but generally higher than 20%, a threshold that is frequently used in the monitoring of cement and resin injections) that, in such saline water saturated soil, can only be due to the massive presence of quasi-insulating solidified matter that has displaced water from the soil pores;
- the columns resulting from bi-fluid jet grouting injections are definitely formed in the upper artificial rubble mound layer, but with a volume that is larger than the expected result in normal soil and with evident accumulation towards the bottom of the accumulated stones, at the interface with the soft loamy sediments that constituted the natural sea floor at the site.
- cross-hole seismic measurements showed significant increases with respect to the normal compressional wave (P) velocity range (1500-1800 m/s) in marine sediments, with average values well above 2000 m/s;
- the ERT measurements were useful to integrate the seismic data and allow to estimate the diameters of the columns that are all in excess of 150 (for columns 3 and 4) and 200 cm (for columns 5,6) (see Fig. 29, red colour in the percent difference images) in the sectors where bi-fluid jet grouting worked successfully;
- the intermediate layer (natural alternation of sandy and silty loose sediments, thickness of approximately 10 meters) is characterized by lateral migration of grout establishing intercommunications between columns;
- the lower clay layer (below 42-44 m depth and ending on top of the bedrock) was treated successfully by bi-fluid jet grouting, resulting in large diameter (over 150 cm) columns

obtained in C4, C5 and C6, while the result obtained in C1 and C2 was similar to what achieved in the intermediate layer; this suggests that the soil heterogeneity is much more significant than expected (from the stratigraphy available) and can play an important role in the success of jet grouting at this site.

5 APPLICATION OF DIAMETER PREDICTION METHODS TO THE RIJEKA CASE

Regarding the six columns of the field trials, the diameter predicted for each soil layer (N0, N1, N2, N3) is calculated.

5.1 METHOD 1

Before starting with the calculations, the model specifies that for columns realized with the bifluid system, the parameters c', tan (phi) and E have to be multiplied for 0.95 (for sands), meanwhile Cu and E for 0.9 (for clays). The following Table 10 show the parameters before and after the correction.

	E (Kpa)	Cu (Kpa)	ϕ (°)
1	/	/	/
N0	30000	/	35
N1	3400	34	22
N2	15000	/	30
N3	4500	45	25
N4	15000	/	32

	E (Kpa)	Cu (Kpa)	ϕ (°)
1	/	/	/
N0	28500	/	33.25
N1	3400	30.6	19.8
N2	14250	/	28.5
N3	4500	40.5	22.5
N4	14250	/	30.4

Table 10 Parameters considered before (left) and after the correction (right)

So, the following values of total and effective stress are determined (approximatively the same for each column, so Table 11 only shows the example of column 1):

		z (m)	σz (kPa)	$u_{hidrost}$ (kPa)	σ'z (kPa)
COLUMN 1	N0	30	471.89	294.3	177.59
	N1	40	668.89	392.4	276.49
	N2	44	745.89	431.64	314.25
	N3	47	803.89	461.07	342.82

Table 11 parameters obtained for z, σz, u and σ'z

The following step is to determine whether a soil is cohesive or granular: from Figure 17 it can be seen that the layers N1 and N3 have Cu values obtained by a triaxial test UU.

For these layers the following parameters are obtained:

$$q_u = 15Cu \tag{41}$$

$$\alpha = 4.5 \tag{42}$$

Meanwhile, for the No and N2 layers (granular soils),

$$q_u = 3\ Kp\ \sigma'_v \tag{43}$$

$$\alpha = 5 \tag{44}$$

Where Kp is the passive earth pressure coefficient.

Considering that the nozzle diameter is 6.5 mm, the η value that is taken is 0.5.
All the values are so shown in the following Table 12.

		qu (kPa)	α	η
COLUMN 1	N0	1965.9213	5	0.5
	N1	510	4.5	0.5
	N2	2828.25	5	0.5
	N3	675	4.5	0.5

Table 12 qu, α, η values for column 1

The following step is finding the value of the erosion radius, using the values obtained until now, and including the injection pressure at the pump Pm (>400 bar for the whole process), following the equation:

$$R_e = -ln\left[\frac{q_u}{\eta P_m}\right] \cdot \frac{1}{\alpha} \tag{45}$$

To obtain the value of E, the parameters obtained from Table 5 for granular soils, meanwhile for cohesive soils the simple relation E=100*Cu is used.

Starting from these relations, the value δ is obtained from the equation:

$$\delta = \frac{(1+\nu)}{E} \cdot q_u \cdot R_e \tag{46}$$

In the next step, it has to be verified if

$$u_f = 2.5\ \sigma_v \tag{47}$$

Is bigger than qu.

This situation is verified only for the layers N0 and N2, where there is a situation of hydraulic fracture: the new values of Re and δ will consider u_f instead of q_u.

Finally, using Eq. (48) and Eq. (49) as follows, the columns' diameters Dc are calculated, obtaining these results (Table 13):

$$D_c = 2(R_e + \delta) \tag{48}$$

$$D_{c,f} = 2(R_f + \delta_f) \tag{49}$$

	Re (m)	δ (m)	uf (kPa)	Rf (m)	δf(m)	Dc (m)
N0	0.464	0.036	1179.725	0.566	0.028	1.188
N1	0.815	0.147	1672.225	/	/	1.924
N2	0.391	0.089	1864.725	0.475	0.075	1.098
N3	0.753	0.143	2009.725	/	/	1.791

Table 13 Re, δ, uf, Rf, δf and diameter results

Considering that all the parameters involved in the model are about geotechnical properties of the soil, and only one about the pressure of injection (which is the same for every column), each column will obtain the same diameter for each layer. That is because the method does not consider the lifting time step ΔT (which was different for every column): that is one of the main parameters which cannot be underestimated, because the bigger the time spent in every step, the bigger will be the diameter.
However, this important parameter is considered in other parts of the calculation, specifically in the C, D and E parts, which evaluate respectively the unit weight of the column and spoil, the cavity pressure, waste slurry pressure and volume of the wasted slurry and finally the total injected volume.
Moreover, in the equations it does not appear (except for an initial reduction coefficient, which has not much influence on the values) the difference between using a monofluid, bifluid or trifluid system.

Considering that soils parameters cannot be changed, the only value which could be modified in the model is the Pm, which needs a pressure of 1500 bar (almost four times bigger than the pressure used) to reach the desired value of 1700mm and 800 bar (twice the pressure used) to reach 1400mm.

5.2 METHOD 2

The two equations used for the diameter calculation are

$$D_a = D_{ref} \cdot \left(\frac{\alpha \cdot \Lambda^* \cdot E'_n}{7.5 \cdot 10} \right)^{\beta} \cdot \left(\frac{N_{SPT}}{10} \right)^{\delta} \tag{50}$$

$$D_a = D_{ref} \cdot \left(\frac{\alpha \cdot \Lambda^* \cdot E'_n}{7.5 \cdot 10} \right)^{\beta} \cdot \left(\frac{q_c}{1.5} \right)^{\delta} \tag{51}$$

Due to the lack of data about the rubble mound (N0) necessary to calculate the q_c and NSPT of that layer, only the results of the layers from N1 to N3 are showed.

Starting from the term E'n, given by the equation

$$E'_n = \frac{\pi}{8} \frac{M \rho d_0^2 v_0^3}{v_s} \tag{52}$$

Considering that not all the parameters are known, it has to be used the alternative formulation, which is calculating the term Ep', given by the equation:

$$E'_p = \frac{pQ}{v_s} \tag{53}$$

With p constant for every column with a value of 400 bar, Q of 426 l/m, the only variable parameter is the lifting speed v_s.

After that, this value is multiplied by 0.9 (which is, according to the author, a reduction given by the distance between the pump and the nozzle) to obtain E'n.

Table 14 shows the results obtained:

		P (kPa)	Q (m^3/s)	Vs (m/s)	E'p (MJ/m)	E'n (MJ/m)
COLUMN 1	N1	40000	0.0071	0.004	64.61	58.149
	N2	40000	0.0071	0.004	64.61	58.149
	N3	40000	0.0071	0.004	64.61	58.149
COLUMN 2	N1	40000	0.0071	0.006	44.02	39.618
	N2	40000	0.0071	0.006	44.02	39.618
	N3	40000	0.0071	0.006	44.02	39.618
COLUMN 3	N1	40000	0.0071	0.007	41.18	37.062
	N2	40000	0.0071	0.007	41.18	37.062
	N3	40000	0.0071	0.007	41.18	37.062

		P (kPa)	Q (m^3/s)	Vs (m/s)	E'p (MJ/m)	E'n (MJ/m)
COLUMN 4	N1	40000	0.0071	0.006	46.15	41.535
	N2	40000	0.0071	0.006	46.15	41.535
	N3	40000	0.0071	0.006	46.15	41.535
COLUMN 5	N1	40000	0.0071	0.004	72.42	65.178
	N2	40000	0.0071	0.004	72.42	65.178
	N3	40000	0.0071	0.004	72.42	65.178
COLUMN 6	N1	40000	0.0071	0.004	79.52	71.568
	N2	40000	0.0071	0.004	79.52	71.568
	N3	40000	0.0071	0.004	79.52	71.568

Table 14 P, Q, vs, E'p and E'n values for each column

According to the model (Figure 30), the value of Λ is given by the relation of water/cement, and considering that in this work ω=1, Λ will be 7.5.

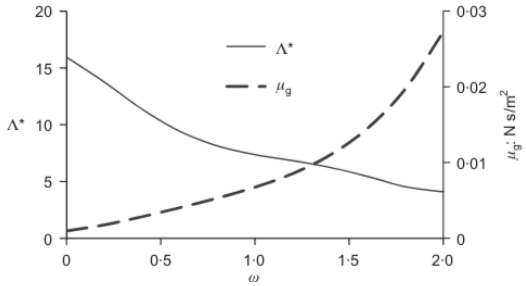

Figure 30 Dependency of Λ* on the composition of grout (ρc 3000 kg/m3); data for μg are taken from Raffle and Greenwood in 1961 (as reported by Bell (1993))

The value α is 6 for the six columns, considering that in the field trials it has always been used a double fluid system.

Once q_c values have been calculated (which this time is expressed as the resistance at the top of the cone in the laboratory test CPTu) with the equation

$$q_c(MPa) = 0.048z\ (m) \tag{54}$$

with z as the quote below the seabed level and having the NSPT values for every layer in the field trials, it will be used a medium value between the ones obtained with the two methods (results showed in Table 15).

		qc (Mpa)	NSPT	Dref (m)	Da qc (m)	Da SPT (m)
COLUMN 1	N1	0.144	2	0.5	1.828	1.521
	N2	0.336	15	0.8	2.366	1.471
	N3	0.48	5	0.5	1.353	1.210
COLUMN 2	N1	0.144	2	0.5	1.693	1.409
	N2	0.336	15	0.8	2.191	1.362
	N3	0.48	5	0.5	1.253	1.121
COLUMN 3	N1	0.144	2	0.5	1.670	1.390
	N2	0.336	15	0.8	2.162	1.344
	N3	0.48	5	0.5	1.236	1.106
COLUMN 4	N1	0.144	2	0.5	1.709	1.422
	N2	0.336	15	0.8	2.212	1.375
	N3	0.48	5	0.5	1.265	1.131
COLUMN 5	N1	0.144	2	0.5	1.870	1.557
	N2	0.336	15	0.8	2.421	1.505
	N3	0.48	5	0.5	1.384	1.238
COLUMN 6	N1	0.144	2	0.5	1.905	1.586
	N2	0.336	15	0.8	2.467	1.533
	N3	0.48	5	0.5	1.410	1.261

Table 15 qc, NSPT, Dref and diameter values for each column

Table 16 shows the values obtained divided per layer and per column type (with expected diameter of 1700mm or 1400mm).

	D (m) (expected 1700 mm)		
	COLUMN 1	COLUMN 5	COLUMN 6
N1	1.675	1.713	1.746
N2	1.919	1.963	2.000
N3	1.281	1.311	1.336

	D (m) (expected 1400 mm)		
	COLUMN 2	COLUMN 3	COLUMN 4
N1	1.551	1.530	1.566
N2	1.777	1.753	1.794
N3	1.187	1.171	1.198

Table 16 Calculated diameter for each column

It is noticed that layer N1 and N2 show very similar results to the ones needed for the project (1.7m for columns 1,5,6 and 1.4m for columns 2,3,4).
N3 is the only layer with a slightly reduced diameter, of approximately 25%, due to the big number of approximation that the method includes, such as the D_{ref} value and the values considered from laboratory test such as the CPTU, considering the q_c value increasing proportionally with depth.

In this method, there are different parameters which can be changed to obtain the desired values, by increasing ΔT and Pm for example.

5.3 METHOD 3

It starts with the calculation of the limit erosion distance XL, which equation is

$$x_L = \frac{\alpha d_0 v_0}{v_L} \tag{55}$$

The value d_0 is already known, being the nozzle diameter of 6.5 mm.
The value of α, given by:

$$\alpha_g = \frac{\alpha_w}{B} \tag{56}$$

Where α_w is considered of 16 by the author, meanwhile B is:

$$B = \sqrt{\frac{\mu_g/\rho_g}{\mu_w/\rho_w}} \tag{57}$$

Where μ_w has a value of 0.001 Pas and ρ_w of 1 kg/m^3, meanwhile μ_g is given by the equation:

$$\mu_g = 0.007(W/C)^{-2} \tag{58}$$

And ρ_g by:

$$\rho_g = \frac{\rho_w \rho_c [1 + (W/C)]}{\rho_w + \rho_c (W/C)} \tag{59}$$

Considering, as said before, the water/cement relation ω=1, we have a value of μ_g=0.007 and so B=2.14

The α found is then calculated by bifluid systems, considering the correction of α for a value ψ, which considers the air pressure of the bifluid system.

$$\alpha_d = \varphi \alpha_g \tag{60}$$

$$\varphi = 1 + 0.054 \frac{p_a}{p_{atm}} \tag{61}$$

Considered for all the columns an air pressure value of approximatively 16 bar, that follows a value of ψ=1.69, and as follows an αd value, showed in Table 17, of:

ALFA						
αw	B	αg	αs	Pa	Ψ	αd
16	2.14	7.4766	7.4766	12.8	1.6912	12.6445

Table 17 Parameters used for the estimation of coefficient α

Beginning later with the critical velocity phase,

$$v_L = \beta \left(\frac{q_u}{p_{atm}} \right)^k \tag{62}$$

Where the β value depends from the granulometry of the different layers, following the equations:

$$\beta = \begin{cases} b_0 \cdot \left(\frac{M_c}{100} \right)^{b_1} \left(\frac{D_{50}}{D_f} \right)^{b_2}, & 5 \le M_c \le 100 \\ b_0 \cdot \left(\frac{5}{100} \right)^{b_1} \left(\frac{D_{50}}{D_f} \right)^{b_2}, & 0 \le M_c \le 5 \end{cases} \tag{63}$$

Due to the lack of data for the granulometry of layer N0, as like in method 2, the calculations won't be done.

Considering that the only layers crossed by the column are N1, N2, N3, it's analyzed the percentage of fine grain M, with values from the report "Book 2 - Vol.2 - Geotechnical Report - doc.1025_M1233", which are respectively 80, 30 and 95%, as it is possible to see in Figure 20.

meanwhile the qu value only depends of the type of soil (granular or cohesive):

-for cohesive soils

$$q_u = 2C_u \tag{64}$$

Where Cu is the undrained shear strength

-for sandy soils

$$q_u = 2\tau_f \tag{65}$$

Where the τ is the shear strength of sand.

And the value of the exponent k which is adimensional is 0.5.

So, the following values of β are showed in Table 18.

		CRITICAL VELOCITY					
		qu (KPa)	MC %	D50 (mm)	Df (mm)	β	VL (m/s)
COLUMN 1	N1	68	75	0.075	0.075	2.558	2.1094093
	N2	181.288	30	0.085	0.075	1.687	2.2707632
	N3	90	95	0.01	0.075	6.295	5.9719629

Table 18 Parameters used for critical velocity estimation

The calculation of the exit velocity with the equation:

$$v_0 = \frac{4Q}{M\pi d_0^2} \tag{66}$$

Considering that all the columns have a Q of 426 l/m, (0.0071 m^3/s) and only one nozzle with constant diameter of 0.0065m, the following values of v_0 are obtained and showed in Table 19.

	EXIT VELOCITY			
	Q (m^3/s)	M	d0 (m)	V0 (m/s)
N1	0.0071	1	0.0065	213.965
N2	0.0071	1	0.0065	213.965
N3	0.0071	1	0.0065	213.965

Table 19 Parameters used for exit velocity estimation

As they only are soil parameters, there is no difference between the columns.
So, the x_L is found for every layer

	V0 (m/s)	VL (m/s)	αd	d0 (m)	XL (m)
N1	213.965	2.109	12.6445	0.0065	8.337
N2	213.965	2.271	12.6445	0.0065	7.744
N3	213.965	5.972	12.6445	0.0065	2.945

Table 20 Parameters used for erosion distance x_L

The last parameter to estimate is the reduction coefficient for erosion distance, given by the equation

$$\eta = a_0 \left(\frac{v_{m0}}{v_m}\right)^{a_1} N^{a_2} \tag{67}$$

Where the parameters N and vm are obtained as follows:

$$v_m = \sqrt{(\pi R_s D_r)^2 + v_s^2} \tag{68}$$

$$N = M \frac{R_s}{v_s} \Delta S_t \tag{69}$$

The results are expressed in Table 21:

		REDUCTION COEFFICIENT							
		vm0 (m/s)	Rs (r/min)	Dr (cm)	Vs (cm/min)	Delta S (cm)	Vm (m/s)	N	η
COLUMN 1	N1	0.071	6.2	7.6	26.374	4	0.025	0.940	0.103
	N2	0.071	6.2	7.6	26.374	4	0.025	0.940	0.103
	N3	0.071	6.1	7.6	26.374	4	0.025	0.925	0.103
COLUMN 2	N1	0.071	8	7.6	38.710	4	0.032	0.827	0.097
	N2	0.071	8	7.6	38.710	4	0.032	0.827	0.097
	N3	0.071	8	7.6	38.710	4	0.032	0.827	0.097
COLUMN 3	N1	0.071	8	7.6	41.379	4	0.033	0.773	0.095
	N2	0.071	8	7.6	41.379	4	0.033	0.773	0.095
	N3	0.071	8	7.6	41.379	4	0.033	0.773	0.095

		REDUCTION COEFFICIENT							
		vm0 (m/s)	Rs (r/min)	Dr (cm)	Vs (cm/min)	Delta S (cm)	Vm (m/s)	N	η
COLUMN 4	N1	0.071	8	7.6	36.923	4	0.032	0.867	0.098
	N2	0.071	8	7.6	36.923	4	0.032	0.867	0.098
	N3	0.071	8	7.6	36.923	4	0.032	0.867	0.098
COLUMN 5	N1	0.071	6.5	7.6	23.529	4	0.026	1.105	0.106
	N2	0.071	6.5	7.6	23.529	4	0.026	1.105	0.106
	N3	0.071	6.5	7.6	23.529	4	0.026	1.105	0.106
COLUMN 6	N1	0.071	6.5	7.6	21.429	4	0.026	1.213	0.108
	N2	0.071	6.5	7.6	21.429	4	0.026	1.213	0.108
	N3	0.071	6.5	7.6	21.429	4	0.026	1.213	0.108

Table 21 Parameters used for reduction coefficient η estimation

Considering all the terms of the equation, the final values for the diameter of the columns are showed in Table 22:

		XL (m)	η	Dr (cm)	D0 (m)
COLUMN 1	N1	8.337	0.103	7.6	1.791
	N2	7.744	0.103	7.6	1.669
	N3	2.945	0.103	7.6	0.681
COLUMN 2	N1	8.337	0.097	7.6	1.688
	N2	7.744	0.097	7.6	1.573
	N3	2.945	0.097	7.6	0.645
COLUMN 3	N1	8.337	0.095	7.6	1.666
	N2	7.744	0.095	7.6	1.553
	N3	2.945	0.095	7.6	0.638

		XL (m)	η	Dr (cm)	D0 (m)
COLUMN 4	N1	8.337	0.098	7.6	1.703
	N2	7.744	0.098	7.6	1.588
	N3	2.945	0.098	7.6	0.651
COLUMN 5	N1	8.337	0.106	7.6	1.837
	N2	7.744	0.106	7.6	1.711
	N3	2.945	0.106	7.6	0.698
COLUMN 6	N1	8.337	0.108	7.6	1.870
	N2	7.744	0.108	7.6	1.743
	N3	2.945	0.108	7.6	0.710

Table 22 Parameters used for diameter estimation

Final diameter results divided per column number and kind are shown in Table 23.

	D (m) (expected 1700 mm)		
	COLUMN 1	COLUMN 5	COLUMN 6
N1	1.791	1.837	1.870
N2	1.669	1.711	1.743
N3	0.681	0.698	0.710

	D (m) (expected 1400 mm)		
	COLUMN 2	COLUMN 3	COLUMN 4
N1	1.688	1.666	1.703
N2	1.573	1.553	1.588
N3	0.645	0.638	0.651

Table 23 Diameter values divided per layer and column

As like for the method studied by Flora, layers N1 and N2 reach the desired values (both for column type 1700mm and 1400mm).
The problem is presented with layer N3, where the results are way lower than expected: as it is possible to seen from Table 22, meanwhile the h and Dr values are the same as the other layers, the erosion distance X_L value is only 2.9 approx. (meanwhile it is more than 7 and 8 m for N1 and N2). This is due to a very high percentage of fines, resulting a high value for β and the critical velocity v_L.

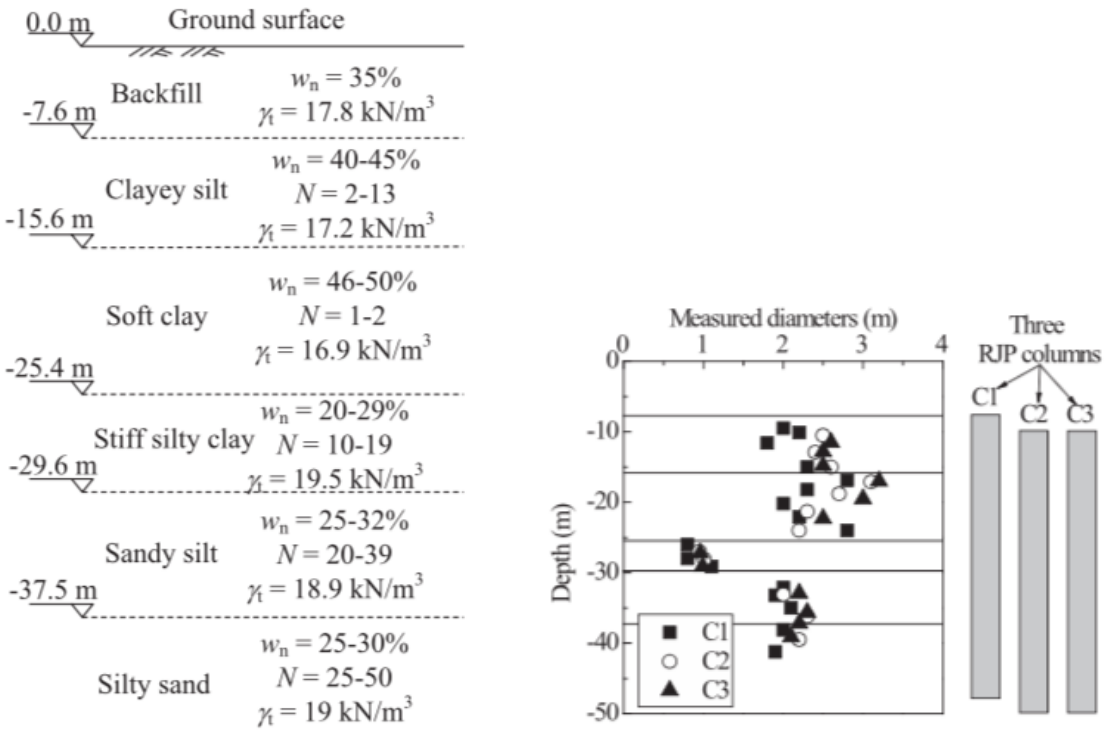

Figure 31 Measured diameters for test columns in Case D (data from Shen et al. 2009b)

The results obtained are coherent with the example given by the author (Figure 31) where the layer of stiff silty clay (similar to N3 layer) gives very low values of the diameter compared to the other layers.

6 ANALYSIS

6.1 COMPARISON BETWEEN METHODS

Figures 32 and 33 shows a comparation between the diameter obtained from the different methods (both for columns planned to be 1700mm and 1400mm):

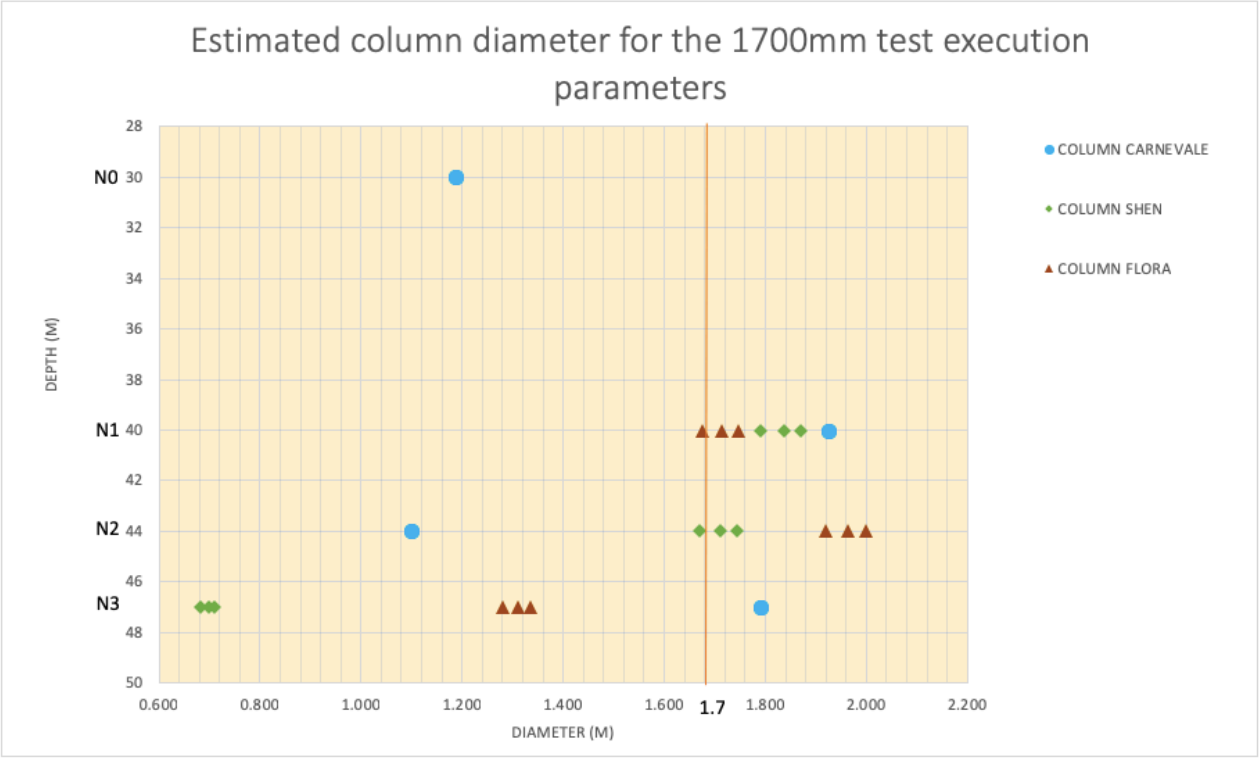

Figure 32 Comparison between the results obtained for each method for columns with expected diameter of 1700mm

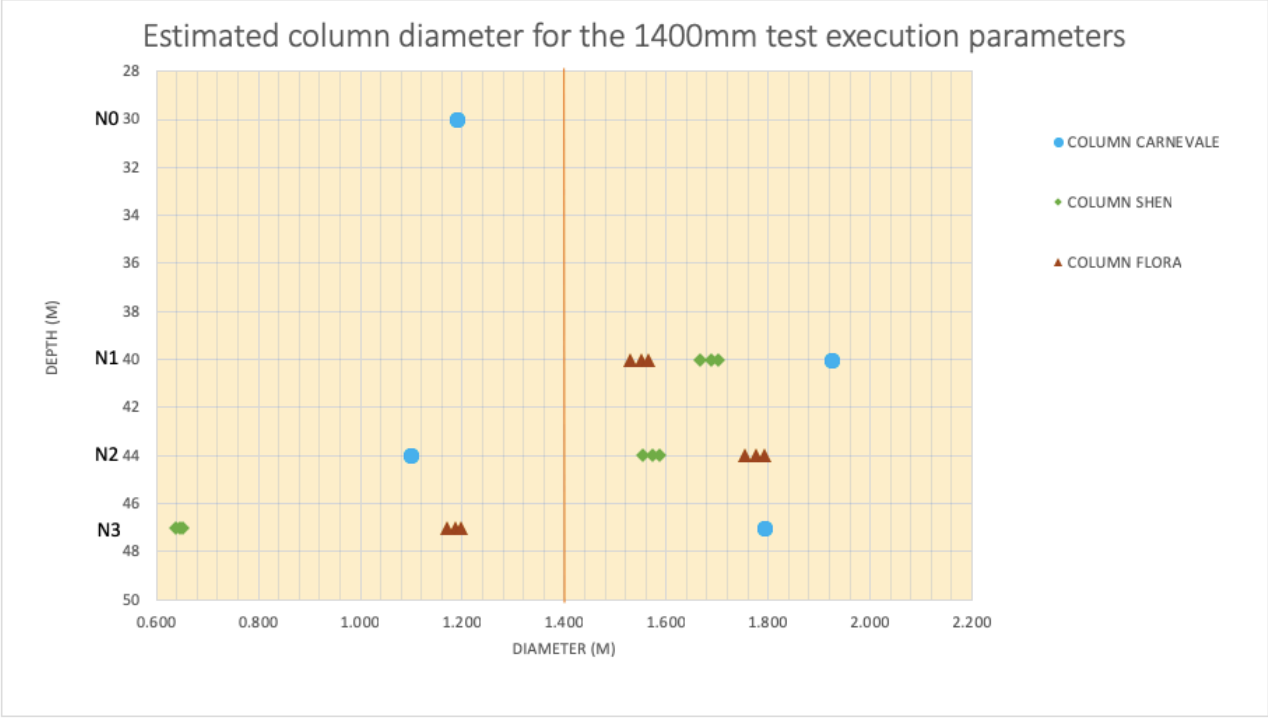

Figure 33 Comparison between the results obtained for each method for columns with expected diameter of 1400mm

-for layer N0 (30m depth) as said before, only the method of Carnevale could be evaluated, as the rubble mound was not possible to fit in the soil categories pre-established for the Flora and Shen methods.
-for layer N1 (sandy clay) we can see that the three methods predict a similar diameter to the target one.

-for layer N2 (carbonaceous sand) Flora and Shen methods produce similar results, slightly above the desired target, meanwhile Carnevale prediction is far below the target value.
-layer N3 (soft clay) is the more interesting. As for the other layers, Carnevale's method predict diameters well above the field target. Flora predicts a small reduction from that target, meanwhile Shen method predicts a very small diameter, due to its sensitivity to granulometry (and as a consequence of its critical velocity) which brings to a big difference for the calculated diameter from other types of soil.

6.2 COMPARISON WITH ERT AND SEISMIC RESULTS

A comparison between results obtained in field trials and with the analytic methods must be done. Reconsidering Figure 29, and the analysis of results made in that chapter, the value of diameter is satisfying from depth of 40m until 50m for columns 3,4,5 and 6, a value that is not represented by the analytical results for layer N3 (47m depth).
Since the soil heterogeneity was not considered between the different columns, all the methods give approximately the same results per layer, so the problem with column 1 and 2 shown in chapter 4.4.3 is not presented within the analytic models.
For the other two layers N1 and N2, the constancy of results shown in Rijeka is similar to the results obtained for the analytic methods.
The method of Carnevale is insensitive to the time step parameter and therefore was unable to distinguish between the different parameters applied in the field trial, predicting the same diameter for all of them. However, the field inspection results showed significant differences due to this execution parameter.
The analytic methods of Flora and Shen showed good results for layer N1 and N2, coherent to the quality tests results, but due to its sensitivity to granulometry (for Shen's method) which result to give a higher critical velocity and due to the parameters' approximations (for Flora's method) discussed in chapter 5.2, the layer N3 presented diameters much lower than expected.
It was not possible to collect enough data for layer N0, because the prediction methods were not calibrated for this kind of material.

7 CONCLUSIONS

A comparison between different analytic methods to predict the diameter of a jet grouting column has been made. The comparison has been based on real data from the Port of Rijeka. It may be concluded that:

All the methods were reasonably consistent in the sandy clay layer but offered very different estimates for the carbonate sands and the soft clay. This may be related to the fact that sandy clay is a very frequently treated material, and the empirical database that supports the methods reflects this fact. On the other hand, carbonate sands are unusual materials. The poor performance of Shen method in the soft clay is somewhat surprising.

There are difficulties in verifying the predictions with the field methods, which are somewhat ambiguous. Therefore, it seems still premature to trust design completely in any of these analytical methods, but they may be useful in planning and interpreting other quality control procedures, like field trials. This is less so for the method of Carnevale, which is insensitive to important execution parameters, like residence time.

Quality control tests have been shown good results: in columns 3,4,5 and 6 the expected diameters (1400 and 1700mm) were reached between 40 and 50m of depth, meanwhile in columns 1 and 2, due to the heterogeneity of the soil and its parameters, the values were way lower.

8 REFERENCES

Arroyo, M., A. Gens, E. Alonso, G. Modoni, and P. Croce. 2007. *"Informes Sobre Tratamientos de Jet Grouting. ADIF LAV Madrid-Barcelona-Francia, Tramo Torrasa-Sants. Report of the Universidad Politecnica de Catalunya"* 110 p [in Spanish].

Bell, A. L. (1993)." Jet grouting. In Ground improvement" (ed. M. P. Moseley), pp. 149–174. Boca Raton, FL, USA: Blackie.

Carnevale, F., Belloni, L. and Grassi, A., 2012 "*Evaluation of diameter and characteristics of jet grouting columns-Analytical approach*" pp. 2061-2067
Geostudi Astier. 2016 "*Cross-Hole Electrical Resistivity Tomography and Seismics monitoring of jet grouting treatment at the Rijeka Harbour test site*" pp. 1-15

Croce, P. & Flora, A. (2000). "Analysis of single fluid jet-grouting". Geotechnique 50, No. 6, 739 – 748

Croce, P., Flora, A., Modoni, G. 2017. "*Jet Grouting Technology, Design and Control*" Editorial CRC Press, pp. 234-250

Flora, A. & Lirer, S. (2011). "*Interventi di consolidamento dei terreni, tecnologie e scelte di progetto (general report)*". Proc. 24th Natl Conf. Geotech Engng 'Innovazione tecnologica nell'Ingegneria Geotecnica', Napoli 1, 87–148 (in Italian).

Flora, A., Modoni, G., Lirer, S. and Croce, P. 2013 "*The diameter of single, double and triple fluid jet grouting columns: prediction method and field trial results*", Géotechnique Volume 63 Issue 11, pp. 935-942

Hinze, J. O. (1948). "*Turbulence, 1st edn*." New York, NY, USA: McGraw-Hill.

Katzenbach, R., A. Weidle, and H. Hoffmann. 2001." *Jet grouting: Chance of risk assessment based on probabilistic methods*", In M. T. Durgunoglu, ed., Proceedings of the 15th ICSMFE, Istanbul, Turkey, August 27–31, 2001: pp. 1763–1766.

Langhorst, O. S., B. J. Schat, J. C. W. M. de Wit, P. J. Bogaards, R. D. Essler, J. Maertens, B. K. J. Obladen, C. F. Bosma, J. J. Seluwaegen, and H. Dekker. "*Design and validation of jet grouting for the Amsterdam Central Station.*" In Geotechniek, Special Number on Madrid XIV European Conference of Soil Mechanics and Foundation Engineering, pp. 20-23. 2007.

Meinhard, K., D. Adam, and R. Lackner. 2010. "*Temperature measurements to determine the diameter of jet-grouted columns*". Proceedings of the International Conference on Geotechnical Challenges in Urban Regeneration, London, United Kingdom, May 26–28: 8 p.

OpusGeo 2014 "*Rijeka Gateway Project Zagreb Pier Container Terminal Phase 1- Main Design- Book 2 Volume 3 – Geotechnical Design*" pp. 3-14, 23-24,

OpusGeo 2014 "*Rijeka Gateway Project Zagreb Pier Container Terminal Phase 1- Main Design- Book 2 Volume 2 – Geotechnical Design*" pp. 23-48

Rajaratnam, N. (1976)". Turbulent jets", Elsevier, Amsterdam, Netherlands.

Shen, S. L., C. Y. Luo, X. C. Xiao, and J. L. Wang. 2009. "*Improvement efficacy of RJP method in Shanghai soft deposit: Advances in ground improvement*"—Research to practice in the United States and China, In J. Han, G. Zheng, V. R. Schaefer, and M. S. Huang, eds., Geotechnical Special Publication 188: pp. 170–178.

Shen, S., Wang, Z., Yang, J and Ho, C. 2013 "*Generalized Approach for Prediction of Jet Grout Column Diameter*" pp.2060-2066

Shibazaki M. (2003). "*State of practice of jet grouting*", Grouting and ground treatment, Geotechnical Special publication No.120, ASCE

Tornaghi, R. (1989). "*Trattamento colonnare dei terreni mediante gettiniezione (jet-grouting)*". Proc. 17th Natl Conf. Geotech. Engng, Taormina 1, 193–203 (in Italian).